International Journal of Biological Macromolecules 340 (2026) 150164

Contents lists available at ScienceDirect

International Journal of Biological Macromolecules

journal homepage: www.elsevier.com/locate/ijbiomac

Addressing bacteria with tannins chemistry: an innovative *food inspired* organic lauryl gallate-based coating to increase probiotics resistance

Mirco Vacca [a,1], Mariasimona Cavaliere [a,1], Giuseppe Celano [a], Daniela Pinto [b], Angelo De Stradis [c], Matteo Spagnuolo [a], Gennaro Brunetti [a], Francesco De Mastro [a], Benito Di Bari [a], Danilo Vona [a,*], Maria De Angelis [a]

[a] Department of Soil, Plant and Food Sciences (Di.S.S.P.A.), University of Bari Aldo Moro, via G. Amendola 165/a, 70126 Bari, Italy
[b] Human Microbiome Advanced Project-HMPA, Giuliani SpA, 20129, Milan, Italy
[c] National Research Council of Italy (CNR), Institute for Sustainable Plant Protection (IPSP), University of Bari, Via Amendola 165/A, 70126, Bari, Italy

ARTICLE INFO

Keywords:
Probiotics
Single-cell coating
Hydrophobic insertion
Lauryl gallate (LG)
Stress resistance
Bioorganic approach
Gastrointestinal survival

ABSTRACT

Functional foods and various applications based on beneficial effect provided by probiotics have gained increasing attention due to the well-established link with human health. Probiotics are pivotally involved in regulating the intestinal microbiota, influencing various physiological processes that impact the overall well-being of hosts. However, ensuring probiotics survival and, after delivery, keeping a residual biological activity remains one of the most major challenges. To address this issue, various encapsulation strategies have been developed to protect probiotics. In this study, we investigated an innovative approach of single-cell coating to enhance cell resistance under stress conditions, including simulated digestion, heat exposure, and refrigerated storage. The methodology employs the natural antioxidant lauryl gallate (LG), entrapped at the molecular level in probiotics membranes *via* hydrophobic insertion, which can be further involved in the synthesis of the macromolecular coating using (and comparing) 3 defined methodologies: oxidative polymerization, cross-linking and metal:organic chelation. All the coated products exhibited the ability to preserve the viability. Our findings demonstrated that coated probiotics showed significantly higher survival rates compared to uncoated controls, particularly under harsh gastric (+2 log) and intestinal conditions (+1 log), as well as during heat treatment (+1.5 log) and long-term cold storage (+3 log). Therefore, the present study highlights the potential of single-cell coatings as an alternative way to encapsulate probiotics enhancing the protection against environmental stressors. These findings provide valuable insights for the development of advanced probiotic delivery systems, including the plausible future applications in functional foods and personalized biomedicine.

1. Introduction

In recent years, consumer interest in nutrition and health has steadily increased, with particular attention given to the potential beneficial properties of foods. In this context, probiotic-enriched foods have been widely recognized for their therapeutic effectiveness in response to a range of impairments and diseases [1,2]. According to the ISAPP [3], probiotics are defined as live microorganisms that confer a health benefit to the host when administered in adequate amounts. Despite their potential effectiveness, conventional oral probiotic preparations face challenges such as reduced activity during production and storage, as well as inactivity in the gastrointestinal environment, resulting in levels below the threshold required to exert benefits [4]. Since at least 1×10^9 viable microbial cells are required to exert positive outcomes in hosts, probiotics viability should be ensured during storage processing, against thermal shock events, and once the gastrointestinal transit is performed right after the administration [5]. Therefore, stabilizing probiotics with suitable excipients, including biocompatible natural matrices and fibers, is essential to enhance their effectiveness and meet the growing consumer demand for foods with high nutritional value and beneficial functional properties. Selection criteria for the resistance and efficacy of probiotics, as well as their safety and metabolic integration with the host, are continually debated among material scientists, microbiologists, food experts, and physicians [6]. To address these issues,

* Corresponding author.
E-mail address: danilo.vona@uniba.it (D. Vona).
[1] These authors equally contributed to the present research.

https://doi.org/10.1016/j.ijbiomac.2026.150164
Received 15 September 2025; Received in revised form 29 December 2025; Accepted 7 January 2026
Available online 8 January 2026
0141-8130/© 2026 Published by Elsevier B.V.

several systems have been developed to increase specific probiotic resistance in particular for the less resilient living microorganisms exhibiting huge beneficial features for human beings [7]. The most suitable and accessible strategy to keep microorganisms unaltered consists on the use of micro- and macro-sized entrapping matrices (capsules, particles, gel) leading to contain and protect bacteria *via* simple *layer-by-layer* deposition of natural biomolecules [8], or confinement in micro-structures [9], or through complex manufacture procedures, such as nuzzling extrusion [10], production of hybrid co-acervates [11], fluidification [12], electro-spraying and chilling [13]. In all these cases, clusters of bacteria can be decorated, surrounded, and protected till the functional target.

A challenging and multidisciplinary field explores the possibility of homogeneously decorating single-cell microorganisms on their surfaces to *armor* bacteria, microalgae, or yeasts against stress conditions, including pH fluctuations, dehydration, or thermal stimuli [14]. The approaches of living cell modifications involve bioorganic chemistry, which gives the opportunity to directly address various functional groups or biomolecules present over cell surfaces [15]. Armoring single cells, rather than cell clusters, offers the advantage of allowing cell replication and preserving over 90% of metabolic pathways, without interfering with *cell-to-cell* interactions. Living cells modified *ad hoc* thus become biohybrids, useful as tools for immunotherapy [16], tissue engineering [17], bioremediation [18] and stem cell confining [19].

From a methodological point of view, the chemical modification of living cells could pass through a bioorganic dual pathway based on the metabolic insertion of a precursor, often followed by an external click reaction [20], leading to decorate and armor cells once they are still living [21–23]. A procedure widely exploited to anchor chemical elements over living cells is represented by the hydrophobic insertion of tailed moieties [24]. The methodology consists of the immobilization on the surfaced bilayer of the plasma membranes of living cells, exploiting medium-high average hydrocarbon chains as interlayer anchors for attaching fluorophores, oligonucleotides, polypeptides, polysaccharides, nanoparticles and organic polymers.

In this research, for the first time, living probiotics have been directly chemically bio-conjugated using a two steps labelling of the external membrane, including first a hydrophobic transient insertion [25] of aliphatic tailed lauryl gallate (LG) in cell membranes and, then, the molecular conversion to a simple tannin-like bioorganic coating to long-lasting decorate living cell surfaces. Once decorated, the cells serve as platforms to initiate *in situ* the production of a tannin-like, fully organic coating thus protecting living cells from harsh conditions. In this context, the trihydroxyphenyl moieties of vicinal gallic acid heads can easily condense *via* direct oxidative polymerization (Fig. 1a), be used to chelate iron ions increasing the steric approach of the aromatic moieties through direct complexation (Fig. 1b) or be esterified with aryl diboronic small molecules to achieve molecular bridging (Fig. 1c).

2. Materials and methods

2.1. Equipment and instruments

Methyl, Ethyl, Isopentyl, Lauryl gallate esters, acetic acid, absolute ethanol, dimethyl sulfoxide, bi-distilled water, tiophene-diboronic acid, m-amino-phenylboronic acid pinacol ester (APB), diethyl 1,4-cyclohexanedione-2,5-dicarboxylate (DCD) were purchased from Sigma Aldrich (St. Louis, Missouri, USA). The micro-FTIR-measurements were recorded using a LUMOS I FTIR spectrophotometer interfaced with a white field microscope, equipped with a video camera, a liquid nitrogen cooled-mercury cadmium telluride (MCT/A) detector, and a computer-controlled mapping stage (OPUS software 2014). Individual spectra were used for peak separation by measuring fields from representative spots, in ATR mode, with a high number of scans to increase the signal-to-noise ratio. Point-by-point spectral mapping of the films was carried out respecting a grid pattern (0.9 × 1.1 mm^2, in quintuplicate fields, 4000–650 cm^{-1} at a spectral resolution of 4 cm^{-1}). An Axiomat, Zeiss microscope (Oberkochen, Germany; DAPI passband λexc: 405 nm; FITC filter exc. 488 nm, em. 520 nm bandpass) was used to record the fluorescence and the surface topography of samples before and after chemical functionalization experiments. ^{1}H NMR experiments with ^{13}C decoupling (and ^{13}C NMR) were performed on a Spinsolve 80 Carbon

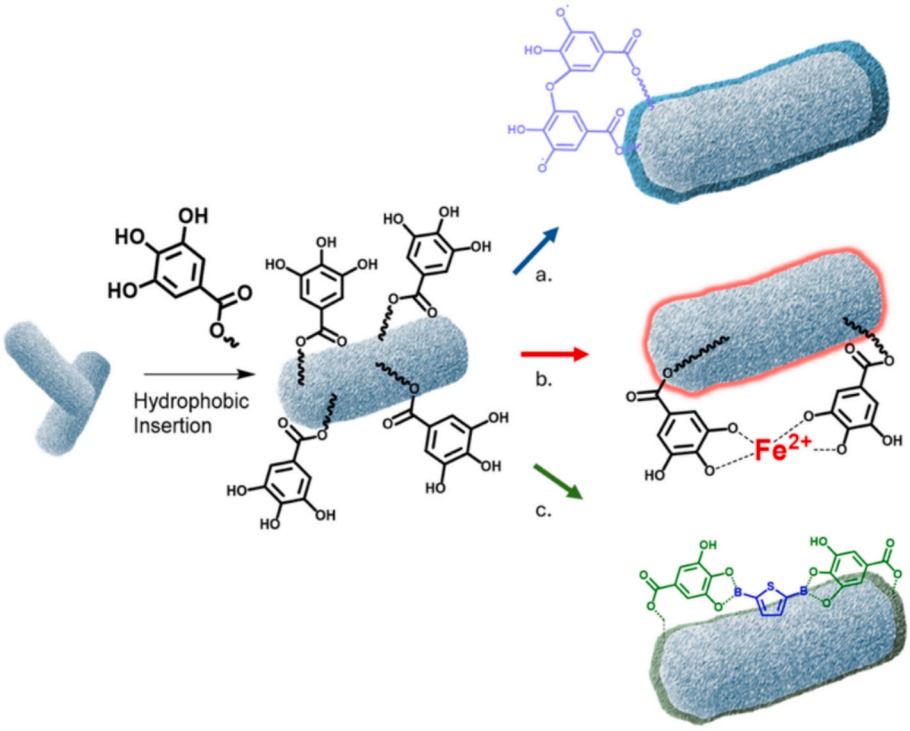


Fig. 1. Scheme reporting hydrophobic insertion of lauryl gallate (LG) and the 3 strategies adopted here to produce stable coatings.

Ultra benchtop NMR spectrometer (Magritek) with a magnetic field strength of 1.88 T (^{1}H Larmor frequency 80 MHz). The ^{1}H NMR experiments were conducted with the following parameters: 6.4 s acquisition time, 16 k data points, 90° excitation pulse, and 32/64 scans. The repetition time was set to 30 s to ensure full pre-magnetization of all components for quantitative analysis. ^{13}C NMR experiment was conducted with 512 scans, 60 s of repetition time.

2.2. Synthesis of compound F

m-amino-phenylboronic acid pinacol ester (APB, 0.8 mM) was added to the ethanol solution (10 mL) containing diethyl 1,4-cyclohexanedione-2,5-dicarboxylate (DCD) (0.42 mmol) and acetic acid (100 μL). The mixture was then refluxed for 16 h under an open-air atmosphere, and the reaction was monitored *via* TLC right after the change of color (from pale yellow to fluorescent orange) [26]. After the reaction, the mixture was cooled down to room temperature, vacuum pumped, and the residual was extracted with bicarbonate aqueous solution (10%) and ethyl acetate (3 × 20 mL). The organic layer was collected, vacuum pumped, and the solid residual was washed with ethanol. The solute dissolved in ethanol was again evaporated and the solid was weighted and characterized *via* ^{1}H NMR and ^{13}C NMR (yield: 69%). The protected pre-F compound was added to the DMSO solution (2 mL) containing HCl-buffered waterish solution (pH 6.3). The mixture was then refluxed for 22 h under an open-air atmosphere, and the reaction was monitored *via* TLC till completion (Fig. 2). After the reaction, the mixture was cooled down to room temperature and utilized as it is for the biological interface.

2.3. Probiotic-model propagation

The probiotic microorganism used in this research was *Limosilactobacillus reuteri* ATCC 23272, thereafter referred as *Ls. reuteri*, which was obtained from the Culture Collection of the Department of Soil, Plant, and Food Sciences (Di.S.S.P.A.) of the University of Bari Aldo Moro. Cells were cultured in de Man, Rogosa, and Sharpe (MRS) broth for 16–18 h at 37 °C to reach the stationary phase, corresponding to a cell density of approximately 10 Log_{10} CFU mL^{-1}, verified both by plate counting and optical density measurement (OD_{620} nm). Before further processing, cells were centrifuged (8000 ×*g* for 10 min), washed twice with an isotonic NaCl solution (0.9 g L^{-1}), and used at final cell density ranging between 7 and 9 Log_{10} CFU mL^{-1}, as properly specified in following subsections.

2.4. Screening for antimicrobial activity

Lauryl gallate (LG) and tannic acid (TA) were screened for their capacity to inhibit viability of *Ls. reuteri*. The detection was based on the agar–spot method described by Tarannum et al. [27], with slight modifications. A fresh culture, MRS for 18 h at 37 °C, of *Ls. reuteri* was used to inoculate 20 mL of MRS agar at the final cell density of approximately 7 Log_{10} CFU mL^{-1}. Wells with a diameter of *ca.* 5 mm were created using a sterile pipette-tips and 50 μL of LG or TA in each well, at different concentration (5–20 μM), were added to each well. Plates were left for 30 min to dry and then incubated at 37 °C for 48 h. Chloramphenicol (Sigma-Aldrich) at the final concentration of 0.01 g L^{-1} and sterile water were used as positive and negative control, respectively. The development of a partial zone of inhibition (0.6–2 cm) was considered as a partial inhibition, whereas a clear zone of inhibition (> 2 cm) around the spot was considered as evidence of positive inhibition.

2.5. Hydrophobic insertion of gallic acid esters

A stock of all the gallic acid esters in ethanol (1 mL, 0.4 mM) was prepared by mixing the solids with the solvent. For the hydrophobic insertion experiment, Methyl, Ethyl, Isopentyl, Lauryl gallate esters, used at final concentration of 20 μM, were incubated at room temperature in MRS broth (pH 6.7 ± 0.2) with *Ls. reuteri* used at a final cell density of 5 × 10^8 cells mL^{-1} (measured *via* OD). The experiment was carried out also at different molecule concentrations (5, 10, 20, 30, 50 μM) and various times (2, 4, 8, 12, 24, 48 h), but the optimized conditions were set with 20 μM for 4 h [28].

2.6. Tannin-like in situ oxidative polymerization for armoring probiotics

For the polymerization test, the experiment was performed in 3 Eppendorf tubes containing 300 μL of MRS broth (pH 6.7 ± 0.2) and a cell suspension (cell density of 3 × 10^8 cells mL^{-1}), to which 60 μL of LG stock solution were added. To the second and third Eppendorf tubes, 15 μL of hydrogen peroxide (H_2O_2) and 30 μL of $NaHCO_3$ solution were added, respectively, to adjust the pH to approximately 8.8. After few minutes of incubation with 100 μg of free GA directly in tubes, the reaction was monitored at 12, 24 and 48 h *via* microscopy and micro-FTIR investigation. Subsequently, a clear color change of the solution was observed, which became between gray and green (Fig. 3).

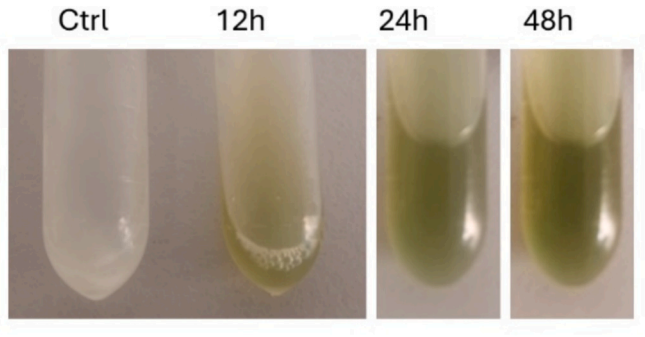


Fig. 3. Color changing during the oxidative polymerization of lauryl gallate inserted in membranes.

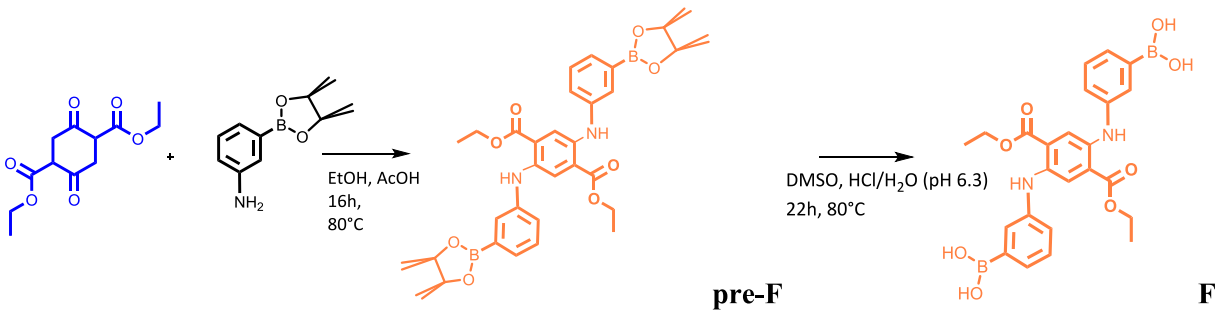


Fig. 2. Reaction scheme for the synthesis of sensor F. **(pre-F):** ^{1}H NMR (500 Mhz, DMSO-D6): *8.1–6.2 (m, 10H), 4.19 (m, 4H), 1.4–0.99 (m, 30 H) ppm.* ^{13}C NMR (500 Mhz, DMSO-D6): 170.56, 151.51, 146.11,135.84, 129.35, 124.54, 121.46, 118.96, 115.29, 112.71, 81.78, 60.42, 24.07, 13.81 *ppm.*

2.7. Tannin-like in situ iron chelation for armoring probiotics

For the iron-chelation, the process started with 20 mL of bacterial culture previously propagated in MRS broth (pH 6.7 ± 0.2) and hydrophobically inserted. This mixture was incubated at 37 °C for 30 min under shaking, favoring the interaction of the compound with the cell membranes and creating the optimal conditions for the subsequent stabilization of the coating. Subsequently, 400 μL of a ferrous nitrate solution in bidistilled water (final concentration of 400 μM) was added and the culture was incubated under the same conditions as before, and the mixture was kept under shaking for additional 19 h at the same temperature. In this approach, ferrous nitrate provides ferrous ions, which stabilize the structure thanks to coordination interactions between LG and TA. This mechanism, distinct from classical polymerization, is in line with previous studies showing how oxidized tannins interact with iron through carboxyl and hydroxyl groups leading to the formation of highly conjugated and stable structures [29]. EDX characterization on bacteria was realized to investigate the presence of Iron complex over bacterial surfaces.

2.8. Tannin-like in situ molecular bridging with bis-boronic-tiophene moiety for armoring probiotics

The mixture of inserted bacteria (kept in MRS broth pH 6.7 ± 0.2) was incubated with 400 μL of TiOF units (free bis-boronic-thiophene bridging core) in ethanol (final concentration: 10 μM), followed by a shaking at room temperature for 19 h. In this approach, TiOF acted as a molecular bridge thanks to its free boronic groups, able to interact with both TA and LG, as well as potentially binding to polysaccharides and membrane proteins. These selective interactions favor the formation of covalent bonds with diol-containing substrates, contributing to the stability and structural integrity of the coating [30].

2.9. Transmission electron microscopy

For each sample, a little drop (20 μL) of suspension was applied to carbon-coated copper/rhodium grid (400 mesh) (TAAB Laboratories Equipment Ltd., Aldermaston, Berks, ENGLAND). The coated grid was floated for 2 min on the drop, rinsed with 0.2 mL of double distilled water, drained off the excess of water by means of a filter paper and analyzed to the electron microscope using a Philips Morgagni 282D transmission electron microscope, operating at 80 kV. Electron micrographs of samples were photographed on Kodak electron microscope film 4489 (kodak Company, New York, USA).

2.10. Efficiency of LG-delivery in culture medium

Liquid chromatography was performed by using a Vanquish Flex UHPLC (Thermo-Fisher, USA) coupled with hESI-Orbitrap Exploris 120 mass spectrometer (Thermo-Fisher, USA). Data acquisition and processing were carried out with Xcalibur 4.0 software (Thermo). Chromatographic separation was carried out on an Agilent C18 poroshell column (4.0 μm) at 40 °C. LG concentration for calibration has been separated by isocratic elution with 0.1% FA in MeOH-ACN (7:3, *v*/v) as mobile phase (100%) with flow speed of 0.35 mL/min, in 15 min run, and with volume of injected sample set at 1 μL. The mass spectrometer was fitted with an electrospray ionization source, and mass detection was carried out in negative ion mode. The conditions for electrospray ionization were set as follows: ion spray voltage: 3.4 KV; source temperature: 325 °C; sheath gas flow rate: 35 L/min; auxiliary gas flow rate: 10 L/min. Data were scanned in full scan-mode in the range of 50–1000 *m/z* with a resolution of 60,000 full width at half-maximum (FWHM). The value range of *M/Z* searched in samples was 337.2022 Da.

2.11. Survival to simulated gastrointestinal transit

Simulated gastric (SGP) and intestinal (SIP) phase accounting for the use of related fluids have been prepared following the method described by Fernández et al. [31] with slight modifications [32]. Bacterial cells were harvested at the stationary phase *via* centrifugation at 8000 ×*g* for 10 min. The pellet was then washed with a physiological NaCl solution (0.9 g L^{-1}) and resuspended in 50 mL of simulated gastric fluid containing NaCl (125 mM), KCl (7 mM), $NaHCO_3$ (45 mM), and pepsin (3 g L^{-1}) (Sigma-Aldrich Co., St. Louis, MO, USA), with the pH adjusted to 2.0. The bacterial suspension was then incubated under anaerobic and stirring conditions at 37 °C for 180 min. Following SGP, the cells were collected and transferred, for SIP, into simulated intestinal juice containing pancreatin (0.1 g L^{-1}) and Oxgall bile salts (0.15 g L^{-1}) (Sigma-Aldrich Co.). The pH was adjusted to 7.0 (±0.2) before incubation at 37 °C under agitation. Samples were collected after further 180 min of incubation. At the end of both SGP and SIP, residual cell density was assessed according to serial dilutions, plating on MRS agar, and incubation at 37 °C for 48 h.

2.12. Storage and thermal resistance

Uncoated (Ctrl) and coated (with lauryl gallate, LG; iron ions, Fe; and thiophene-based diboronic acid, Tio) probiotics were subjected to refrigerated storage (4 ± 2 °C) until 21 days and heat-tolerance at 50 and 55 °C for 30 min [9]. Thereafter, probiotic cells (coated and Ctrl) were added in test tubes containing saline solution (NaCl 0.9 g L^{-1}) and, according to ten-fold serial dilutions, plated on MRS agar (37 °C for 48 h) to assess the residual cell viability (Log_{10} CFU mL^{-1}).

3. Results and discussion

The manipulation of living cells surface often opens perspectives to control specific cell behavior, including cell-to-cell interaction, cell-environment responses, division and protection from harsh conditions. Hydrophobic insertion of aliphatic tailed small molecules, or polymers and nanoparticles, has been revealed as a robust and elegant approach to selectively decorate cell membranes. Although there are some impressive results *in vitro*, several obstacles remain to a broader application of some of these strategies. The choice of the tailed moieties, together with the exposition timings, and the homogeneity in surface distribution, become crucial parameters to take account on [24]. For our specific experimental setup, lauryl (dodecyl) gallate (LG) was used directly to interact with cell membranes of bacteria. LG is an ester derivative of gallic acid (GA) being the natural plant triphenol. LG and the other derivatives of GA, *i.e.*, methyl-, propyl-, octyl-gallates, are widely used as antioxidants in the food manufacturing as well as in the pharmaceutical, cosmetic industries, acting as scavengers of reactive oxygen species (ROS) [33], and surface decorating organic moieties for environmental remediation [34]. Owing to the antioxidant activity, LG protects mitochondrial functions of eukaryotic cells and specifically human red blood cells against oxidative stresses [35]. After the insertion of LG, several biomembranes became resistant to peroxidation and metabolic disturbances or integrity damage. This effect is due to the LG ability to scavenge radicals and to its inhibition of the enzyme responsible for the peroxidation process [36]. Moreover, the antioxidant activity of LG can deeply penetrate into phospholipid bilayer during its hydrophobic insertion, so the increase in length of the aliphatic tail augments the possibility to protect LG, being incorporated, concentrated, and exerting biological effects [25,37].

Thinking on an applicative outcome in probiotics, the Maximum Permitted Level (MPL) for gallates (E312), including lauryl (dodecyl) gallate (LG), are established in Annex II of Regulation (EC) No 1333/2008 [38,39] on food additives. Hence, in the European Union, LG is authorized for use within the MPL of 25–400 mg/kg. Although data focusing on LG specifically in human intestinal models remain limited,

relevant insights derived from studies on gallic acid (GA) and related alkyl-gallates. The work carried out by Yang et al. ([40]) summarized evidence indicating that GA can exert beneficial effects on gut health by modulating gut microbiota and enhancing short-chain fatty acid (SCFA) synthesis. This led to benefits strengthening intestinal barrier integrity while attenuating inflammation, as also supported by data obtained from animal models of colitis [41]. These effects are mediated, at least in part, through immune and redox-regulatory pathways. Importantly, GA supplementation was associated with an increased abundance of beneficial taxa, including lactobacilli, without presenting evidence of adverse intestinal effects at nutritionally relevant doses. Wang et al. ([42]) demonstrated that alkyl-gallates are stable in the gastric environment, reaching the small and the large intestine where undergo to controlled hydrolysis by intestinal lipases and gut microorganisms resulting in a conspicuous release of free GA in distal tracts of the large intestine. This behavior supports a prolonged intestinal exposure to GA. Noteworthhy, microbial hydrolysis occurred without impairing bacterial viability, suggesting the occurrence of a presumptive compatibility of this molecule with probiotic growth and metabolic activity. Consistently, *Streptococcus thermophilus* CHCC 3534 adapted to GA exhibited an increased β-galactosidase metabolism, a condition that enhanced its antagonistic activity against intestinal pathogens such as *Escherichia coli* O157:H7 and *Listeria monocytogenes*, indicating that GA can also contribute to improve the potential benefits associated to probiotics administration. Therefore, these findings support the food-grade claim of LG and suggest that its intake cannot lead to adverse effects on gut microbiota providing a plausible mechanistic basis allowing us to speculate about a minimal interference of LG against probiotic growth/survival and organic acid metabolism.

3.1. Hydrophobic insertion of polyphenol

The present investigation began by evaluating the hydrophobic insertion of 4 GA-esters (methyl, ethyl, isopentyl, lauryl gallate) at a concentration of 20 μM in ethanol:water 1:95, in contact with probiotics, used at a cell density of 3×10^8 cells mL^{-1}, for 4 h. The aim of this first approach is to find the correlation among the length of the hydrophobic tail of the esters and the capacity of performing the membrane insertion. The evaluation of the inserted gallic moiety has been performed recurring to a staining protocol based on a newly synthesized aryl di-boronic moiety. As reported in literature [43], aryl boronic molecules can be esterified with vicinal diols of sugars or bi- and tri-phenol groups at mild biological conditions, and this reaction can be exploited to stain these functionalities over biological cells or tissues. Our single benzene dye, synthetized as reported, and characterized, bears a double boronic functionality and has luminescent properties with a shaded yellow/orange emission. Once the hydrophobic insertion of gallic acid esters into probiotic bacteria had taken place, and the stock of aryl boronic had been prepared in DMSO-buffered water, the hydrophobically *inserted* bacteria and the control bacteria were incubated for 4 h with the molecule in final phosphate buffer 50 mM pH 7.4, 20 μM dye. The concentration of the boronic sensor is so low that it does not create extracellular deposition or artefact interference. The bacteria were deposited on a slide, dried, and observed in two-dimensional fluorescence microscopy with a cube/dichroic FITC filter (exc. 488 nm, em. 520 nm bandpass). This allowed us to observe, the clear permanence of the diboronic sensor on the surface of the probiotic bacteria (Fig. 4a), likely due to the formation of the boronic ester with the vicinity diols present on the cell surface of both saccharides and

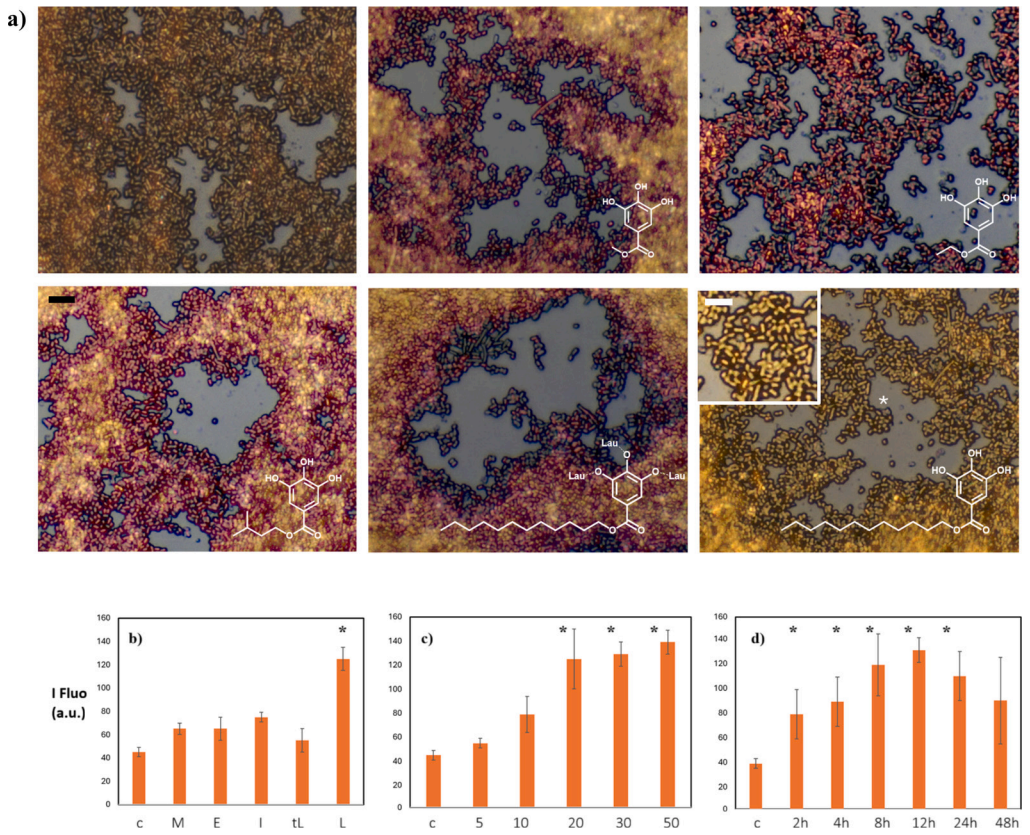


Fig. 4. Length evaluation of aliphatic tailed gallate esters: (a) fluorescence micro-graphs (inset reveals bacteria morphology, general scale bar: 50 μm; inset scale bar: 20 μm); (b) histograms of luminescence intensity depending on type of chemistry (M, Methyl-; E, Ethyl-; I, Isopentyl-, tL, Lauryl gallate-tetra-ester, L, Lauryl gallate mono-ester) of insertion; (c) dependence of luminescence intensity and LG concentration (μM) (See Supp. Fig. S1); (d) dependence of luminescence intensity and exposition time. Statistical evaluation (Anova Bonferroni; * means a *p*-value <0.05): b) significance for ctrl *vs* Lau; c) significance for ctrl *vs* Lau 20, 30, 50; d) significance for ctrl *vs* all other samples (with exception of 48 h).

gallic acid-based moieties. The rod-shaped morphological profiles morphological profiles of microorganisms were perfectly visible.

The covalent staining agent is always present in all samples, including the control (Ctrl), and that in the monomer LG-based inserts there are high intensity profiles (Fig. 4a), with uniformity of color and intensity itself. The sensing of bisboronic derivative also led to distinguish various degrees of insertion based on the molecular weight of the hydrophobic tail of the esters. The control sample exhibits fluorescence as the local diols present in the glycocalyx and on the peptidoglycan of the cell wall appear on the surface. For a specific sample, however, in which the tris-lauryl gallate of the anhydride was added, we expect that the insertion has certainly occurred, but as there are no other sites with available free diols, no substantial improvement is observed compared to the other samples. From this test it can therefore be stated that LG makes a hydrophobic insertion into the plasmatic membrane of lactobacilli, and then we can proceed with the polymerization test. In terms of LG concentration and exposition timing of bacteria with LG solutions (Fig. 4b–d), the optimum for LG resulted as 20 μM in concentration and 2–4 h in time. These outcomes are the direct consequence of some literature statements and demonstration about these types of molecules: the hydrophobic insertion of LG has been already demonstrated for artificial membranes reconstitution and their colloidal investigation [37], while lauryl-based tails have been added to organic fluorophores aiming to integrate photoluminescence properties directly across membranes of living cells [44].

Lauryl gallate is an amphiphilic molecule with a triphenolic polar head and a hydrophobic aliphatic tail. The interaction of the polar head groups is repulsive when partially dissociated, resulting in a pH-dependent push-pull behavior, while the aliphatic tails interact by hydrophobic exclusion in preformed cell membranes. This is mainly because LG is not added at a critical micellar concentration sufficient to cause pre-micelling in solution. Reaching membranes, especially in lipid bilayers, these types of molecules provoke a flipping planarization increasing an interlayer order thus stabilizing directly in membranes. Although the tails are perfectly packed, the external polar head groups can maintain their redox reactivity and acid-base properties, contributing to subsequent chemical rearrangements.

3.2. Efficiency of LG-delivery in culture medium

LG-decorated bacteria were collected *via* centrifugation at different times right after the hydrophobic insertion (1, 2, 4, 8, 12 h corresponding to D1–D5 fractions, respectively) to test the delivery of the compound in the bacterial media (Supp. Fig. S2). The supernatant was solvent-solvent extracted using methanol:ethyl acetate:acetonitrile (8:1:1) from the waterish samples. This organic layer was then analyzed *via* high resolution LC-MS, after defining a calibration curve for 0–40 μM L^{-1} of LG. After the investigation, the D1 fraction (1 h delivery), here considered giving a value of insertion efficiency, was found to contain 45% above the total LG added (20 μM) reaching 55% of inserted LG above the total. D2 and D3 (2, 4 h) were found giving 0.1 and 0.01 μM, respectively, while D4 and D5 exhibited a delivered concentration undetectable standing down the LOQ for LG.

3.3. On cell derivatization of inserted polyphenol using 3 bioorganic strategies

Once the hydrophobic insertion of LG on the surface of the model bacteria studied was verified, the *on-cell* derivatization reactions of the GA head were exploited to produce an armoring (oligomer or polymer-based) coating of the biological elements. Cells inserted here serve as platforms for the *in-situ* production of a fully organic tannin-like coating, designed to protect living cells from harsh conditions. *De facto*, a certain susceptibility of the triphenol moiety protruding outside living cells to dissociate could make it capable to direct interact (electrostatically) with cation heads of phospholipids, while the packed aliphatic tails thermodinamically stabilize. Therefore, the molecular lock of LG comes from 2 different processes: electrostatics with phospholipids, block of cell uptake due to highly polar functional groups of the head. Therefore, the locked trihydroxy groups of vicinal GA can: *a.* easily undergo oxidative polymerization through direct condensation; *b.* chelate iron ions to enhance the steric interaction of the aromatic groups through direct complexation; or *c.* be esterified with small aryl di-boronic molecules, resulting in molecular bridging.

For the process *a.*, the oxidation and auto-oxidation of GA in alkaline aqueous solutions have been studied for a long time given the large presence of GA and its derivatives in food products. Among the possible conversions that can occur during the processing of food and drinks in which GA can be found is the formation of polymers. To allow polymerization, the use of a radical activator is necessary. Among the various methods studied to induce polymerization, the enzymatic route exploiting horseradish peroxidase (HRP) is well established, or, as done in the study, the effect of deprotonation of GA in solutions with alkaline pH and hydroxyl radical (OH●) homolysis product of H_2O_2. The reaction between the peroxyl radical and the gallate dianion, stable at a pH value higher than 7.8, leads to the formation of gallate radical which can proceed to subsequent reactions including oxidation and autoxidation reactions [45]. From the polymerization of GA there is evidence of the formation of greenish compounds that not only present new C—O bonds, but also C—C bonds.

To verify the ability to produce functional tannin-based coatings starting from inserted bacteria, a sample of labeled bacteria was enriched with free GA, which acted as an exogenous molecule initiating polymerization, in contact with a small portion of basic solution of sodium hydrogen carbonate and hydrogen peroxide. The polymerization times evaluated were 12, 24 and 48 h, and the investigations were carried out *via* two-dimensional fluorescence microscopy (DAPI cube/dichroic filter bandpass exc. 365 nm, Fig. 5) and FT-IR microscopy in mapping mode (Fig. 6). Compared to the control sample, microscopy revealed blue scattering fluorescence for samples cured at 12, 24, and 48 h (Fig. 5), and this blue fluorescence is probably due to LG oligomers with -C-O-C- and -C-C- conjugation systems between two hydroxyphenyl units.

The sample subjected to 12 h of incubation was considered optimal by a morphological point of view, the formation of quasi-monolayers on observation glasses, and the absence of organic clustering induced by functionalization.

The different samples were subjected to μFT-IR mapping to characterize their macromolecular bulk (Fig. 6). Since the blank analysis was carried out with air and not on the slide, in all the spectra (especially for 0 and 12 h) a band at around 3300 cm^{-1} can be seen, which represents the stretching of the O—H bond of the silanol groups present on the surface of the slide and in cytosolic and surface water that has not been completely removed. It is appropriate to assume that the addition of GA and other molecular sources of –OH groups, including carbohydrates present on bacteria, do not influence the intensity of the peak. Furthermore, in all the spectra, the peak of the stretching of the -C=O carbonyl at around 1650 cm^{-1} and the bending of the -N-H at around 1550–1600 cm^{-1} are noted. These two peaks largely depend on the peptides that belong to the protein bulks of the bacteria. However, a progressive lowering of these peaks is noted compared to a peak present at 1350 cm^{-1} which greatly exceeds the carbonyl stretching peak in the last spectra set. The peak most likely represents the asymmetric stretching of the C-O-C bond of the ethers formed by the polymerization of gallic acid (Fig. 6). The signal immediately preceding and partially covered by the asymmetric stretching peak is the symmetric stretching peak of the same bond.

Another interesting peak is located at around 700 cm^{-1}. This is already visible in the second spectrum, and it grows considerably up to the fourth graph. Although the area below 1000 cm^{-1} is difficult to interpret given the large overlap of peaks, we can hypothesize that the sharp peak represents the *out-of-plane bending* of the hydrogens bound to

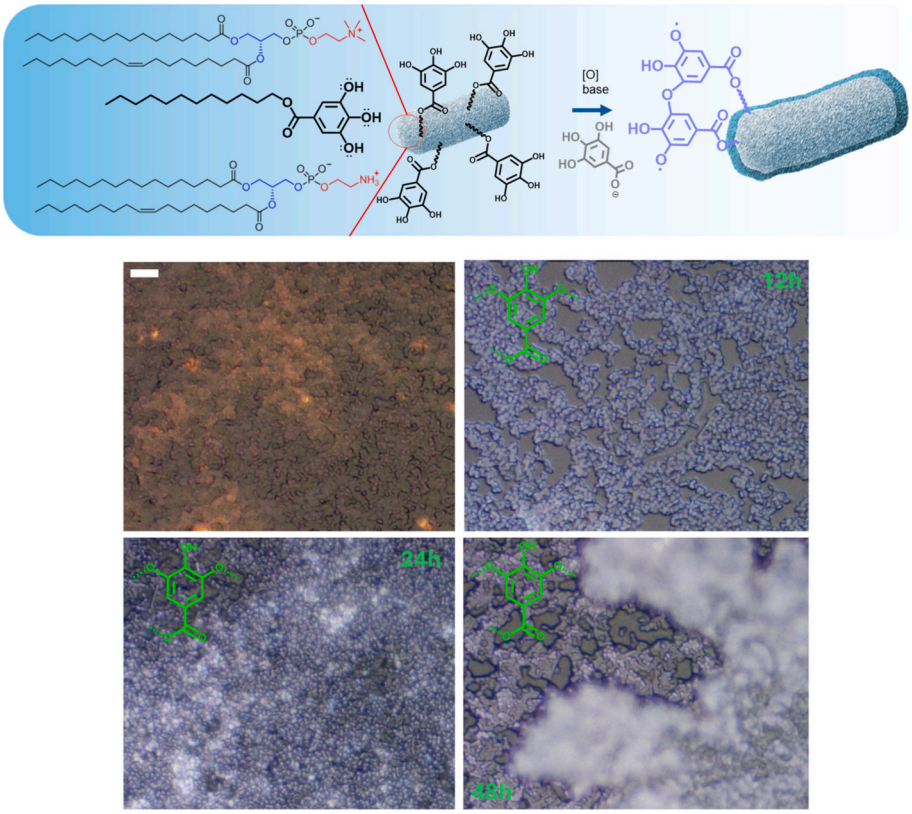


Fig. 5. Up: schematization of the electrostatic lock of LG and its packing into membranes. Down: Two-dimensional fluorescence microscopy (DAPI cube/dichroic filter bandpass exc. 365 nm, scale bar: 100 μm) to evaluate the presence of tannin-like polymer coatings.

the aromatic ring present in the GA polymers formed. Based on data obtained by observing the spectra, we conclude that the polymerization of GA induced on the surface of the lactobacilli successfully occurred.

It was possible to parameterize the relative decrease in the intensity of the -NH bending peaks belonging to proteins, with respect to the relative increase in the intensity of the peaks belonging to the ether-type covalent bonds (-C-O-C-, new polymer). As shown and reported in the Fig. 6, ratios range from an average value of 3.0 setting finally to 0.39. This decrease has been caused by the increasing presence (time-dependent) of oxygenated aryl moieties following oxidative polymerization.

Tannic acid (TA) is a remarkable naturally occurring polyphenol, celebrated for its ability to form complexes with metal ions. This unique property enables the formation of coordination networks through the self-assembly of TA and metal ions, resulting in the creation of metal-phenolic networks. These composites establish stable yet dynamic structures that can be expertly engineered or customized for targeted therapeutic applications. Synthetic metal:organic tannic complexes are specifically designed to modify various biointerfaces, leveraging their exceptional physicochemical properties. These include universal adhesion, pH responsiveness, adjustable size and stiffness, straightforward preparation, and outstanding biocompatibility. Such attributes make them extremely advantageous for a wide range of biological applications, particularly in the field of the cell therapy [46].

For the process *b.*, chelate iron ions, from the water soluble iron (II) nitrate, have been *on cell* synthesized to sterically approach the aromatic moieties of the inserted polyphenols *via* direct complexation, as reported in literature *ad hoc* to perform coatings on living yeast cells [47]. Unfortunately, this complexation process leads to produce molecular quasi-monolayers, which are difficult to characterize using conventional spectroscopic techniques due to the thickness of layer or organic matrix and the absence of distinctive probe-functional groups. Herein, surface EDX technique has been exploited to correlate iron percentage, expressed as Fe/C signal, with the exposition time of iron (II) nitrate with the living probiotics. Among 0.1, 0.25 and 0.5 h of exposition time, and avoiding a certain mortality of cells, we chose 0.5 h exposition time to investigate the biological effects of the coatings (Fig. 7).

The third synthetic polyphenol proposed in this scientific work presents innovative features compared to similar coatings already exploited in literature. The TA reported provide coverage on probiotic biological systems that pass through nanoprecipitation over living cells surfaces *via* metal chelation [48] or electrostatic sandwich technique [49], in which TA is the negatively charged polyelectrolyte interfacing with positively bearing moieties. The intervention, here in our last case, of a covalent, click bioorganic approach that begins with a hydrophobic insertion and ends with organo-metalation and bridging, plays a crucial role in increasing the temporal performance of the coatings, diminishing the time of the polymerization procedure and avoiding the use of toxic metal sources, as in the case of Iron chelation. The method *c.* consists of the use of tiophene-based diboronic acid, approved by FDA, capable of an ester cyclization and related bridging of the protruding polyphenol heads of inserted LG over the cell surfaces. Again, this covalent bridging process results in the formation of molecular quasi-monolayers still difficult to characterize using classical spectroscopic techniques, due to the low thickness. By the way, benchtop ^{1}H NMR simulation [50] here has been propose to simulate *in vitro* the reaction and monitor it by peaking the di-phenol:boronic ester moiety (Fig. 8). The intervention of a bridging process between free boronic moieties and free catechol functionalities aims to produce an intramolecular bi-ester, which dramatically changes the reciprocal ratio between the intensity signals of -OH/aromatic bulk in gallic acid methyl ester (as reported for the monitored reaction in Supp. Fig. S3).

3.4. Transmission Electron Microscopy (TEM) characterization

The three polymer composites grown around the peptidoglycan layer of naked, non-chemically decorated bacteria (Fig. 9a, a-focus) form

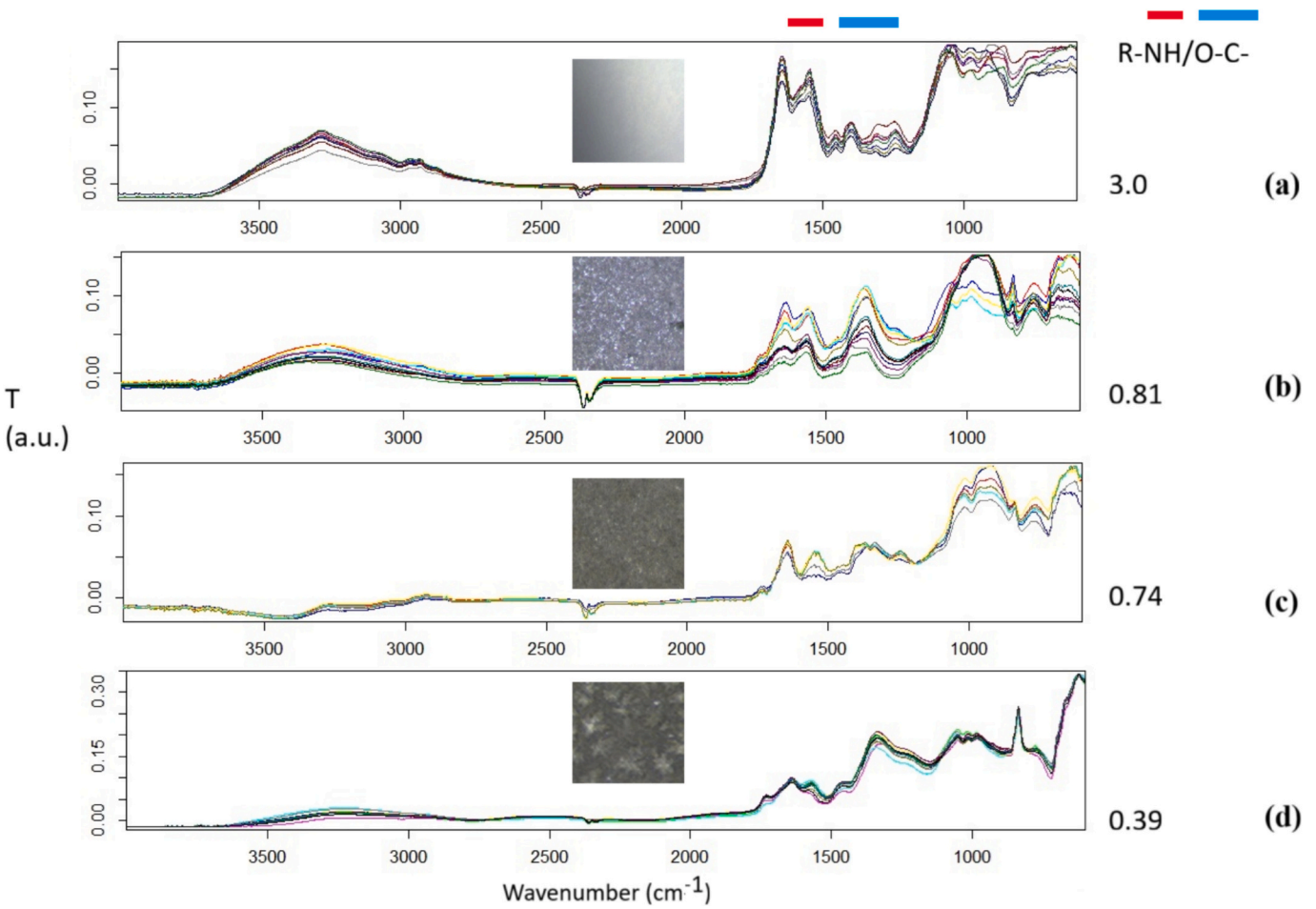


Fig. 6. Characterization *via* μFT-IR microscopy in mapping mode of bare cells (a), and 12 h- (b), 24 h- (c) 48 h- (d) coated living cells. Squares represent 1/10 of the analyzed surface area (1 mm × 1 mm).

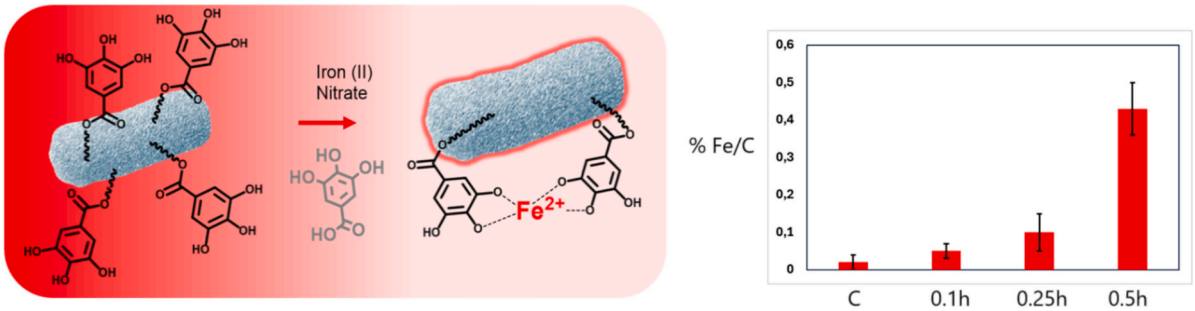


Fig. 7. EDX characterization of iron-chelate gallate coated living bacteria after 0.1, 0.25 and 0.5 h of exposition. Statistical evaluation (Anova Bonferroni): significance reached for ctrl *vs.* 0.5 h (p-value <0.05).

completely different submicroscopic structures. In this context, transmission electron microscopy (TEM) helps us to qualitatively define the three depositions performed. In Fig. 9b, b-focus, it is possible to observe how the oxidative polymerization of the gallic acid heads produces hair-like systems typical of many organic polymers grown *in situ*. Fig. 9c, c-focus, shows the lamellar, flat, two-dimensional systems easily shown also by small organometallic molecules which aggregate at biological interfaces, such as Fe:GA complexes. Finally, molecular bridging with bis-boronic protruding ends leads to cloudy structures that protrude around individual bacterial cells (Fig. 9d, d-focus). TEM microscopy therefore reveals how the supramolecular structuring and hierarchization of identical molecules, in this case LG, can change by simply changing the reaction conditions and the chemical nature of the ligand (*e.g.*, iron for chelation and organoboron for bridging).

3.5. Cell susceptibility to monomers and polymers

According to the optimal layer formation as coating on the probiotic cell wall, and before proceeding with the validation of the coating bioactivity in terms of cell viability protection, the potentially antimicrobial and/or cytotoxic activity of both monomers (LG) and polymers (TA) was assessed on plates. This assay was grounded in evidence that polyphenols can either inhibit or promote microbial growth, including the lactic acid bacteria (LAB), depending on their concentration and

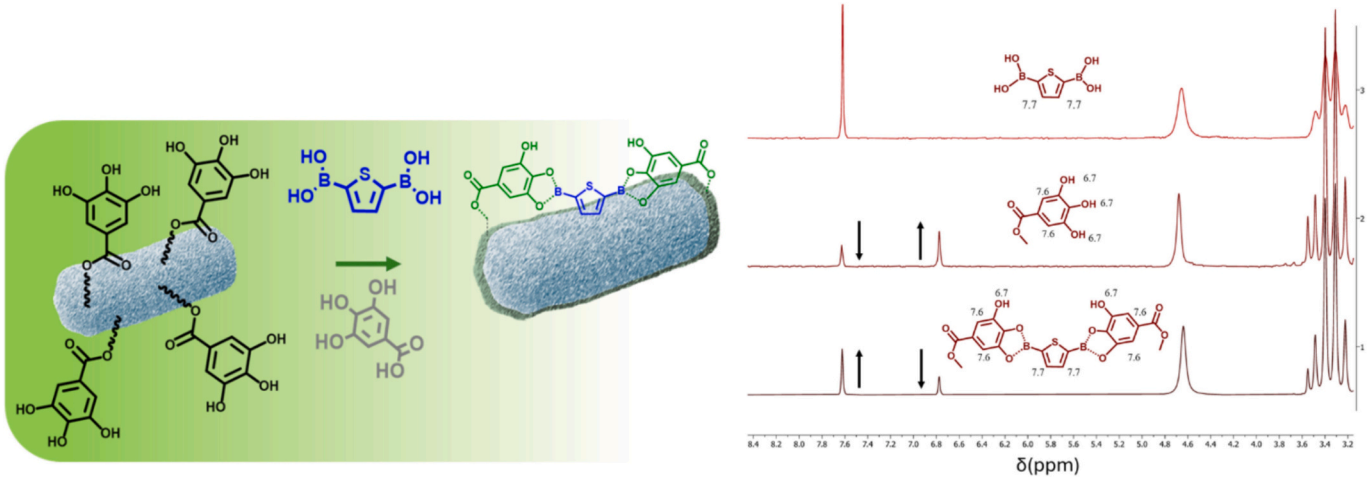


Fig. 8. ^{1}H NMR characterization of the intramolecular bis-boronic based ester with gallic acid methyl ester.

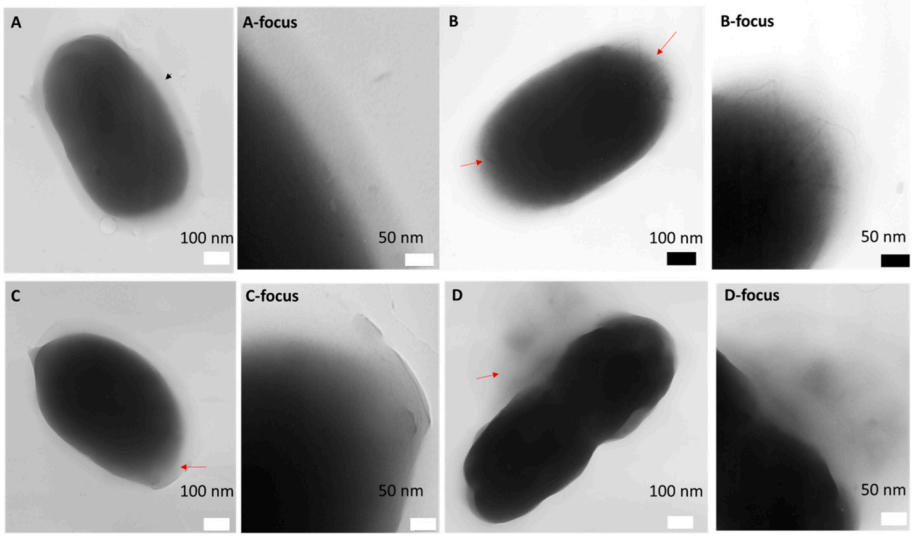


Fig. 9. TEM characterization of bare bacteria (A, focus), and bacteria covered with LG polymer (B, focus), LG:iron chelate (C, focus) and diLG bridged with bis-boronic moiety (D, focus). Scale bar for A, B, C, D: 100 nm. Scale bar for focus pictures: 50 nm.

composition [51,52]. Therefore, before investigating how processing time and how phases directly influence probiotic viability, this assessment was conducted to rule out the possibility of direct cell inhibition by TA and/or LG at the working concentrations used. The molecular diffusion assay was performed using different concentrations (5–20 μM) of the LG monomer (Supp. Fig. S4a) and the TA polymer (Supp. Fig. S4b). No inhibition zones were observed in either the negative control (C−) or at any of the tested molecule concentrations. In contrast, the inhibition zone around the positive control well (C+) exceeded 2 cm, confirming the validity of the assay and the suitability of using of the chosen working concentration of LG at 20 μM.

3.6. Probiotics viability during processing

Trends in cell viability were studied throughout the entire processing (Fig. 10), from the hydrophobic insertion phase to the end of the molecule polymerization phase. Starting from an initial cell density of 8 Log_{10} CFU mL^{-1} (T0), no significant differences were observed in probiotic cell density after 30 min of hydrophobic insertion (HI), as well as after the additional 30 min of processing required for the experimental conditions involving iron ions (Fe) and thiophene-based diboronic acid (Tio). The absence of significant differences aligns with our previous

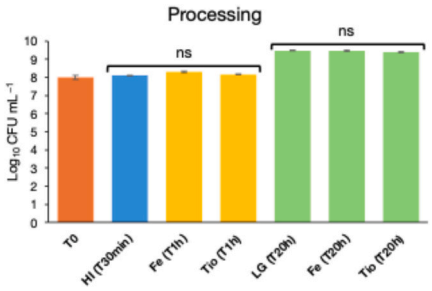


Fig. 10. Cell viability during the processing of three different experimental conditions of coating: lauryl gallate (LG), iron ions (Fe), and thiophene-based diboronic acid (Tio). Starting from an initial probiotic cell density (T0), all experimental conditions (LG, Fe, and Tio) underwent hydrophobic insertion (HI) for 30 min. In the Tio and Fe conditions, an additional 30-min processing phase followed (T1). Regardless of the experimental condition, all samples underwent a total processing time of 20 h (T20). Stacked bars show the mean values (±SD) of three biological replicates (three technical replicates each). "ns" on stacked bars corresponds to "not significant" (p-value > 0.05; two-tailed Student's t-test).

results on antimicrobial and/or cytotoxic activity highlighting the absence of inhibitory activity from LG monomers. Moreover, short time processing (0.5–1 h) did not represent an adverse condition having the potential risk of reducing the cell viability. Noteworthy, instead, the subsequent processing time, required to achieve the polymerization-based coating, showed an increase in cell viability (~9 Logs) in all experiments (LG, Fe, Tio), without differences based on the different nanoarmor strategy. As demonstrated by Pan et al. [53], probiotics can be individually protected using a biocompatible supramolecular coating based on tannic acid (TA) and ferric ions. According to *in vitro* experiments, the application of this nanoarmor strategy enhanced the bacterial viability under acidic gastric simulated conditions. Thus, in mouse models, the designed coating allowed an increased intestinal colonization preserving the microbial proliferation, a condition that represents a pivotal driver for the use of probiotics and essential to allow over time the exploitation of the healthy functions for which these were selected. In line with this, previous authors have stated, indeed, that single-cell armoring allowing the cell replication [54] and the preservation of the microbial metabolic activity without interfering with *cell-to-cell* interactions [55] represents an additional way to design future probiotics with improved healthy functions.

3.7. Probiotics viability in harsh conditions

3.7.1. Simulated digestion

Coated probiotics underwent simulated digestion (Fig. 11). Residual viability was assessed after both the simulated gastric and intestinal phases (SGP and SIP, respectively) and compared to uncoated cells used at the same initial density (Ctrl). Previous studies have highlighted the importance of gastrointestinal resistance in probiotic selection [56–58] due to a high number of potentially suitable probiotics that fail to maintain adequate viability under these conditions [59]. A significant decrease of approximately 2 Log_{10} (CFU mL^{-1}) was, indeed, observed in Ctrl cells following SGP, with further reduction to 6.5 ± 0.4 Logs after SIP. As expected, given its large application as a commercial probiotic, the *Ls. reuteri* used in this study maintained a moderate residual viability despite the exposure to adverse abiotic factors during SGP. Although lactic acid bacteria (LAB) are intrinsically tolerant to acidic environments, it is noteworthy that all three experimental coating conditions preserved a residual viability of 9 Logs after SGP, with final densities of approximately 7.5 Logs only after SIP. From a functional perspective, this represents a significant outcome for the development of probiotic-enriched foods, as it suggests that lower supplementation levels could be required to ensure sufficient cell densities for gut colonization [5]. Notably, slight differences were observed among the experimental conditions, with LG- and Fe-coated cells showing significantly higher viability than Ctrl, whereas Tio-coated cells did not differ significantly from the uncoated Ctrl.

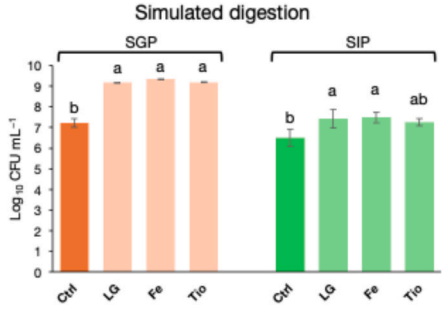


Fig. 11. Cell viability during simulated digestion. Probiotics, either uncoated (control, Ctrl) or coated with different experimental treatments (lauryl gallate, LG; iron ions, Fe; and thiophene-based diboronic acid, Tio), were tested for resistance to simulated gastric and intestinal phases (SGP and SIP, respectively). Stacked bars represent the mean values (±SD) of two biological replicates (3 technical replicates each), with different superscript letters indicating significant differences (p-value <0.05; two-tailed Student's t-test).

3.7.2. Stress conditions: heating and storage

Since high temperatures can affect membrane fluidity, compromising cellular integrity and basic cell processes [60], coated probiotics were also assayed for resistance to heat stress at 50 °C and 55 °C for 30 min (Fig. 12). Although an intermediate ability of *Ls. reuteri* to resist to middle heating conditions was known, as previously confirmed by its persistence in natural whey starter [61], a slight lost in cell viability was observed in the control samples (Ctrl, uncoated), with significant decreases of 1.2 Log_{10} (CFU mL^{-1}) and 1.5 Log at 50 °C and 55 °C, respectively. Notably, coated cells, regardless of the type of coating (LG, Fe, or Tio), exhibited a minimal and not significant decrease in cell density that did not exceed 0.2 Log at 50 °C. Moreover, although residual cell densities at 55 °C were slightly lower than those found at 50 °C, viability loss of coated cells remained limited, with reductions of 0.5 Log in LG and Fe-coated cells and 0.8 Log in Tio-coated cells, with a decrease exceeding the significance threshold in the condition with Tio-based coating only. Previous studies, despite using different coating approaches, reported similar protective effects. For instance, microencapsulated *Ls. reuteri* maintained viability even after dilution in infant formula at 70 °C, with a reduction of only 1 Log [62]. Similarly, Liu et al. observed a 1 Log of decrease in *Lactiplantibacillus plantarum* coated with zein nanoparticles and pectin when exposed to 65 °C for 10 and 30 min [63]. These findings support the effectiveness of single-cell coatings in enhancing the thermal stability of probiotics.

Designed for potential application in future functional foods containing viable probiotics, coated cells were also tested for resistance to refrigerated storage (4 ± 2 °C) for up to 21 days, with an intermediate evaluation at 8 days (Fig. 13). A significant decrease in cell viability was observed in the control samples (Ctrl, uncoated), with reductions of 0.8 Log_{10} CFU mL^{-1} after 8 days and 3 Log_{10} CFU mL^{-1} after 21 days. Several factors can negatively impact probiotic viability during storage, including the diffusion of intracellular oxygen species, reduced nutrient availability, exposure to light, relative humidity, autolysis processes, and water loss [54]. Notably, in this study, we aimed to develop a more sustainable and energy-efficient approach, avoiding lyophilization and similar preservation techniques [64,65] that are commonly used to extend probiotic viability. Despite the absence of these stabilization processes, our coating effectively preserved probiotic cell density for up to 8 days. While a slight but not significant decline was observed at 21 days, survival under refrigeration remained notably higher than in the Ctrl group, with losses not exceeding 1 Log_{10} CFU mL^{-1} compared to the related starting values of cell density. Therefore, this suggests a strong potential for its application in functional foods, ensuring higher probiotic viability over time while reducing energy expenditure associated with conventional stabilization methods. Among the experimental conditions, although differences were not statistically significant, LG-coated probiotics exhibited the highest residual viability, whereas the Tio-based coating resulted in the lowest.

While the bridging method is simple, fast, and convenient as a click chemistry process, with a 1:1 functional clicking ratio, the effectiveness of using cyclic boronic esters formed on vicinal diols is limited to certain pH values and the presence of various external stressors (such as temperature changes). This would certainly explain why C-O-C covalent bonds formed during the oxidative polymerization process and iron-chelation are likely more convenient when the microbiological hybrid system must be subjected to deleterious stresses.

The different protective performances observed among the three coating strategies can be rationalized according to the distinct physicochemical properties, supramolecular architectures, and bond stabilities of the resulting coatings. Although all coatings originate from the same LG-precursor, oxidative polymerization, metal–phenolic chelation, and boronic ester bridging generate fundamentally different interfacial structures that modulate stress resistance through complementary

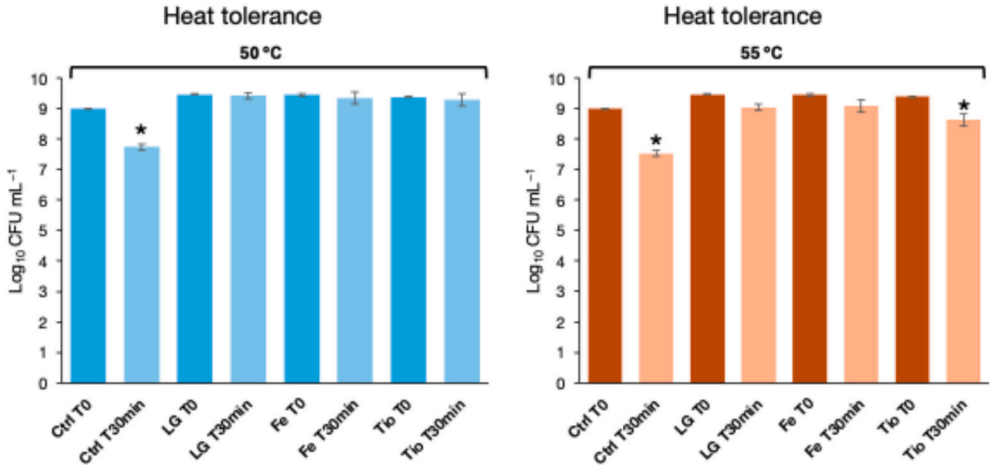


Fig. 12. Cell viability after heating conditions. Probiotics, either uncoated (control, Ctrl) or coated with different experimental treatments (lauryl gallate, LG; iron ions, Fe; and thiophene-based diboronic acid, Tio), were tested for resistance to heating-based stress conditions at 50 and 55 °C, both for 30 min. Stacked bars represent the mean values (±SD) of two biological replicates (3 technical replicates each), with asterisks (*) indicating a significant difference (p-value <0.05; two-tailed Student's t-test) compared to the related starting value of cell density.

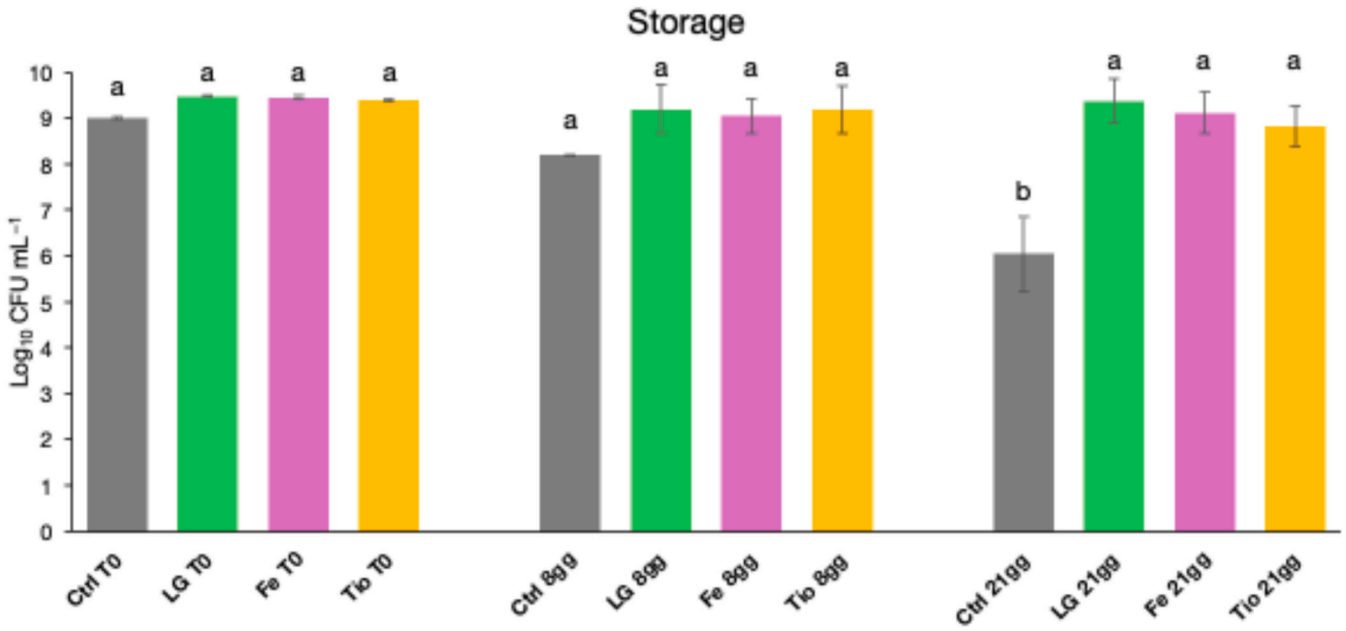


Fig. 13. Cell viability during storage. Probiotics, either uncoated (control, Ctrl) or coated with different experimental treatments (lauryl gallate, LG; iron ions, Fe; and thiophene-based diboronic acid, Tio), were tested for resistance to storage at 4 °C until 21 days. Stacked bars represent the mean values (±SD) of two biological replicates (3 technical replicates each), with different superscript letters ($^{a–b}$) indicating a significant difference (p-value <0.05; two-tailed Student's t-test).

mechanisms. Oxidative polymerization of GA moieties yields a covalently crosslinked tannin-like network, as evidenced by μFT-IR analysis and TEM imaging, forming a dense yet flexible polymeric layer around individual cells. This network likely acts as a semi-permeable diffusion barrier, limiting acid species penetration during gastric exposure, reducing oxidative damage, and stabilizing membrane fluidity under thermal stress, as previously reported for polyphenol-based and polydopamine coatings on probiotics [53,54]. The higher resistance observed under simulated gastrointestinal and storage conditions for LG-polymer–coated cells is therefore consistent with the formation of robust C—C and C–O–C bonds that remain stable across a broad pH and temperature range. In contrast, iron-mediated chelation produces metal–phenolic coordination networks characterized by lamellar, two-dimensional structures. These coatings provide effective short-term protection by increasing steric hindrance and buffering local pH changes, in line with previous studies on Fe–tannic acid nanoarmors [46,47]. However, their partially reversible coordination chemistry may render them more sensitive to prolonged storage or extreme thermal stress, explaining the intermediate performance observed. Finally, boronic ester–based molecular bridging generates thinner, quasi-monolayer coatings stabilized by reversible covalent bonds between boronic acids and vicinal diols. While this strategy ensures rapid coating formation and preserves cell viability during processing, boronic ester linkages are known to be pH- and temperature-sensitive, particularly under acidic or fluctuating conditions [30]. This intrinsic chemical reversibility likely accounts for the comparatively lower protective effect of the Tio-based coating during gastrointestinal simulation and heat exposure. Therefore, collectively, these results highlight that probiotic protection is not solely determined by coating presence but is strongly influenced by coating chemistry, bond stability, and supramolecular

organization.

3.8. Industrial translation, safety, and practical challenges

Currently, LG is authorized as a food additive within the EU, with a MPL ranging from 25 to 400 mg/kg, thus, supporting its food-grade safety when used within regulatory limits. One of the main challenges associated with the scalability and industrial implementation of a LG–based coating concerns its potential interactions with components of the food matrix. It is well established that polyphenols, including gallic acid esters, can form complexes with proteins, carbohydrates, and lipids, thereby influencing the chemical, technological, and sensory properties of foods [66]. Interactions between polyphenols and polysaccharides may alter viscosity, gelling behavior, and system stability, affecting the structure of the final product [67]. Likewise, interactions with proteins—mediated by hydrophobic interactions, hydrogen bonding, van der Waals forces, or covalent bonds—can modify solubility, gelation capacity, and protein functionality, with potential consequences for texture and digestibility [68]. These interactions may also lead to sensory changes, such as increased astringency, bitterness, or color modifications associated with the formation of pigmented complexes [66]. Another critical aspect is the stability of polyphenols during industrial processing, including heating, pH fluctuations, and prolonged storage, which may compromise antioxidant activity or promote chemical degradation. Under an applied perspective of view, this condition could reduce coating integrity leading to a premature and uncontrolled probiotic release within the food matrix impairing the bacterial viability. From a safety perspective, these effects emphasize the need for the process optimization to ensure consistent performance during the product shelf life. Beyond experimental relevance, the proposed LG-mediated bioorganic coating strategy may find direct translation into industrial applications. The use of food-grade reagents, mild processing conditions, and solvent-free or low-energy steps supports scalability and compatibility with existing production lines, potentially limiting additional manufacturing costs. Hence, potential applications can include refrigerated functional foods, non-lyophilized supplements, and beverage-based probiotics products, where maintaining microbial viability sometimes remains challenging. Future works should therefore address pilot-scale validation, techno-economic assessment, sensory acceptance testing, and regulatory alignment to facilitate the transition from laboratory-scale proof-of-concept to validated formulations with higher Technology Readiness Levels.

4. Conclusions

In all the studied cases, the production of a surface resistant spanned fully organic matrix inspired by natural antioxidants was assessed. As in the first-mentioned case, with the polymerization, or in following two, with the synthesis of oligomer-based capsules, the polyphenol was blocked over cell surface of the living probiotics working to armor probiotics for multiple technological applications as well as for direct administration to hosts.

The comparison of this current scientific work with others presenting single-cell armoring (with polydopamine, with spore-inspired nanocoats and polyphenols, with silica:polymers electrostatic sandwich) reveals a competitive outcome in terms of increase of log of probiotics after GI transit (Fig. 14). This data, together with the ease with which hybrid systems are synthesized, the low cost of the monomers, and the usable mild reaction conditions, make the approach technologically integrable and universally applicable.

Beyond the experimental relevance, the approach here presented may find direct translation into several industrial applications. The ability to confer enhanced resistance to probiotics through bioorganic coatings, as in this case through LG-mediated strategies, offers potential value for the food and nutraceutical sectors since the methods described herein are compatible with mild processing conditions and food-grade reagents, making them suitable for integration into existing production lines with limited adjustments. Their potential applications include the formulation of refrigerated functional foods, non-lyophilized supplements, or beverage-based probiotic carriers where viability over time is challenging. Thus, future work may explore pilot-scale validation, cost-benefit analysis, and regulatory alignment to support the transition from bench to market. Thus, these findings represent a step forward toward the development of next-generation probiotic formulations that combine efficacy, stability, and sustainability.

CRediT authorship contribution statement

Mirco Vacca: Writing – original draft, Visualization, Software, Methodology, Investigation, Formal analysis, Data curation, Conceptualization. **Mariasimona Cavaliere:** Writing – original draft, Investigation, Data curation. **Giuseppe Celano:** Writing – review & editing, Validation, Methodology, Investigation, Formal analysis. **Daniela Pinto:** Writing – review & editing, Validation, Resources. **Angelo De Stradis:** Methodology, Investigation, Formal analysis. **Matteo Spagnuolo:** Writing – review & editing, Resources, Project administration. **Gennaro Brunetti:** Writing – review & editing, Validation. **Francesco**

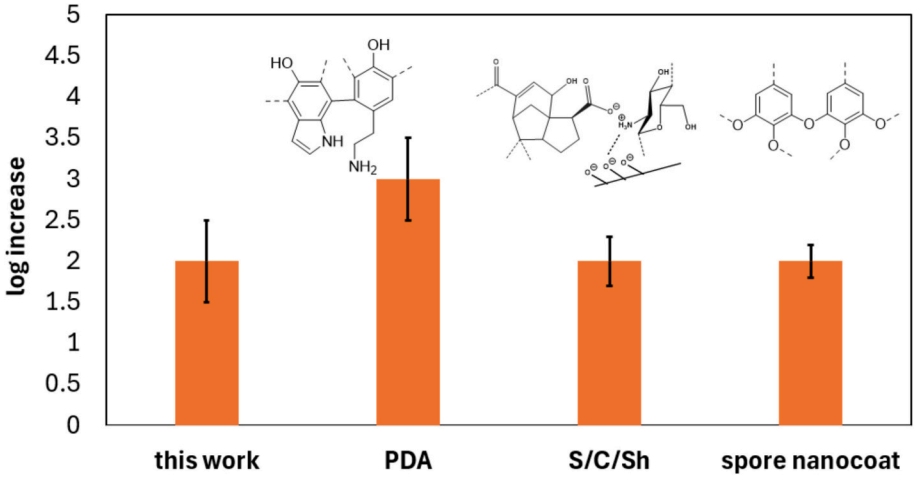


Fig. 14. Histograms related to a comparison of the performance of the coating proposed in the current work, in terms of log increase of bacteria after GI transit of probiotics, with other polymer-based single cell armoring methodologies: with polydopamine [69], with Silica/Chitosan/Shellac [9], with spore nanocoatings and other polyphenol-based protocols [53,70].

De Mastro: Writing – review & editing, Supervision, Resources. **Benito Di Bari:** Investigation. **Danilo Vona:** Writing – original draft, Visualization, Validation, Software, Methodology, Investigation, Formal analysis, Data curation, Conceptualization. **Maria De Angelis:** Writing – review & editing, Validation, Supervision, Resources, Project administration, Funding acquisition.

Funding

This research was funded under the National Recovery and Resilience Plan (NRRP), Mission 4-'Education and Research', Component 2-'From Research to Business', Investment 1.4-'Strengthening research structures and creating R&D' national champions 'on specific key enabling technologies (Agritech)', CUP: H93C22000440007, code: CN_00000022, and by OnFoods, Project code PE00000003, Concession Decree No. 1550 of 11 October 2022 adopted by the Italian Ministry of University and Research, CUP H93C22000630001, Project title 'ON Foods – Research and innovation network on food and nutrition Sustainability, Safety and Security – Working ON Foods'. This research was also supported by "PEC 4 FRESH – ERC SEEDS UNIBA" (D.R. n. 2667 of 14.07.2023) CUP: H93C23000640001.

Declaration of competing interest

Daniela Pinto was employed by Giuliani S.p.A. Other authors declare no conflict of interest.

Acknowledgements

The authors would acknowledge Giuliani S.p.A. for supporting the research activity of Mariasimona Cavaliere.

Appendix A. Supplementary data

Supplementary data to this article can be found online at https://doi.org/10.1016/j.ijbiomac.2026.150164.

Data availability

All raw data supporting the findings of this study are available on request to the corresponding author.

References

[1] A.C. Bunge, A. Wood, A. Halloran, L.J. Gordon, A systematic scoping review of the sustainability of vertical farming, plant-based alternatives, food delivery services and blockchain in food systems, Nat. Food 3 (2022) 933–941, https://doi.org/10.1038/s43016-022-00622-8.

[2] A. Tzachor, C.E. Richards, L. Holt, Future foods for risk-resilient diets, Nat. Food 2 (2021) 326–329, https://doi.org/10.1038/s43016-021-00269-x.

[3] C. Hill, F. Guarner, G. Reid, G.R. Gibson, D.J. Merenstein, B. Pot, L. Morelli, R. B. Canani, H.J. Flint, S. Salminen, P.C. Calder, M.E. Sanders, The International Scientific Association for Probiotics and Prebiotics consensus statement on the scope and appropriate use of the term probiotic, Nat. Rev. Gastroenterol. Hepatol. 11 (2014) 506–514, https://doi.org/10.1038/nrgastro.2014.66.

[4] V. D'Amico, M. Cavaliere, M. Ivone, C. Lacassia, G. Celano, M. Vacca, F.M. La Forgia, S. Fontana, M. De Angelis, N. Denora, A.A. Lopedota, Microencapsulation of probiotics for enhanced stability and health benefits in dairy functional foods: a focus on pasta Filata cheese, Pharmaceutics 17 (2025) 185, https://doi.org/10.3390/pharmaceutics17020185.

[5] A. Terpou, A. Papadaki, I. Lappa, V. Kachrimanidou, L. Bosnea, N. Kopsahelis, Probiotics in food systems: significance and emerging strategies towards improved viability and delivery of enhanced beneficial value, Nutrients 11 (2019) 1591, https://doi.org/10.3390/nu11071591.

[6] S. Parvez, K.A. Malik, S. Ah Kang, H.-Y. Kim, Probiotics and their fermented food products are beneficial for health, J. Appl. Microbiol. 100 (2006) 1171–1185, https://doi.org/10.1111/j.1365-2672.2006.02963.x.

[7] M. De Araújo Etchepare, G.L. Nunes, B.R. Nicoloso, J.S. Barin, E.M. Moraes Flores, R. De Oliveira Mello, C. Ragagnin De Menezes, Improvement of the viability of encapsulated probiotics using whey proteins, LWT 117 (2020) 108601, https://doi.org/10.1016/j.lwt.2019.108601.

[8] W. Krasaekoopt, S. Watcharapoka, Effect of addition of inulin and galactooligosaccharide on the survival of microencapsulated probiotics in alginate beads coated with chitosan in simulated digestive system, yogurt and fruit juice, LWT Food Sci. Technol. 57 (2014) 761–766, https://doi.org/10.1016/j.lwt.2014.01.037.

[9] D. Vona, S.R. Cicco, F.M. La Forgia, M. Vacca, A. Porrelli, G. Caggiano, M. De Angelis, L. Gesualdo, G.M. Farinola, All bio-based μ-beads from microalgae for probiotics delivery, Adv. Sustainable Syst. 2400384 (2024), https://doi.org/10.1002/adsu.202400384.

[10] J.P. Boerman, C.L. Preseault, A.L. Lock, Effect of dietary antioxidant and increasing corn oil inclusion on milk fat yield and fatty acid composition in dairy cattle, J. Dairy Sci. 97 (2014) 7697–7705, https://doi.org/10.3168/jds.2013-7701.

[11] J. Van Wijk, J.W.O. Salari, N. Zaquen, J. Meuldijk, B. Klumperman, Poly(methyl methacrylate)–silica microcapsules synthesized by templating Pickering emulsion droplets, J. Mater. Chem. B 1 (2013) 2394, https://doi.org/10.1039/c3tb20175a.

[12] B. Haffner, R. F., Diab, A. Pasc, SRSMC UMR 7565, Université de Lorraine, CNRS, Bd des Aiguillettes-BP 70239 F-54506 Vandœuvre-lès-Nancy, France, Encapsulation of probiotics: insights into academic and industrial approaches, AIMS Mater. Sci. 3 (2016) 114–136, https://doi.org/10.3934/matersci.2016.1.114.

[13] A.K. Niamah, S.T. Gddoa Al-Sahlany, S.A. Ibrahim, D.K. Verma, M. Thakur, S. Singh, A.R. Patel, C.N. Aguilar, G.L. Utama, Electro-hydrodynamic processing for encapsulation of probiotics: a review on recent trends, technological development, challenges and future prospect, Food Biosci. 44 (2021) 101458, https://doi.org/10.1016/j.fbio.2021.101458.

[14] X. Yang, C. Wang, Q. Wang, Z. Zhang, W. Nie, L. Shang, Armored probiotics for oral delivery, Smart Med. 2 (2023) e20230019, https://doi.org/10.1002/SMMD.20230019.

[15] P.F. van Swieten, M.A. Leeuwenburgh, B.M. Kessler, H.S. Overkleeft, Bioorthogonal organic chemistry in living cells: novel strategies for labeling biomolecules, Org. Biomol. Chem. 3 (2005) 20, https://doi.org/10.1039/b412558d.

[16] X.Z. Zhou, K.P. Lu, The isomerase PIN1 controls numerous cancer-driving pathways and is a unique drug target, Nat. Rev. Cancer 16 (2016) 463–478, https://doi.org/10.1038/nrc.2016.49.

[17] S.T. Laughlin, C.R. Bertozzi, Imaging the glycome, Proc. Natl. Acad. Sci. USA 106 (2009) 12–17, https://doi.org/10.1073/pnas.0811481106.

[18] D. Vona, S.R. Cicco, R. Ragni, C. Vicente-Garcia, G. Leone, M.M. Giangregorio, F. Palumbo, E. Altamura, G.M. Farinola, Polydopamine coating of living diatom microalgae, Photochem. Photobiol. Sci. 21 (2022) 949–958, https://doi.org/10.1007/s43630-022-00185-4.

[19] D.Y. Lee, B.-H. Cha, M. Jung, A.S. Kim, D.A. Bull, Y.-W. Won, Cell surface engineering and application in cell delivery to heart diseases, J. Biol. Eng. 12 (2018) 28, https://doi.org/10.1186/s13036-018-0123-6.

[20] E.M. Sletten, C.R. Bertozzi, Bioorthogonal chemistry: fishing for selectivity in a sea of functionality, Angew. Chem. Int. Ed. 48 (2009) 6974–6998, https://doi.org/10.1002/anie.200900942.

[21] G. Buscemi, D. Vona, R. Ragni, R. Comparelli, M. Trotta, F. Milano, G.M. Farinola, Polydopamine/ethylenediamine nanoparticles embedding a photosynthetic bacterial reaction center for efficient photocurrent generation, Adv. Sustainable Syst. 5 (2021) 2000303, https://doi.org/10.1002/adsu.202000303.

[22] J.H. Jeong, J.J. Schmidt, R.E. Kohman, A.T. Zill, R.J. DeVolder, C.E. Smith, M.-H. Lai, A. Shkumatov, T.W. Jensen, L.G. Schook, S.C. Zimmerman, H. Kong, Leukocyte-mimicking stem cell delivery via in situ coating of cells with a bioactive Hyperbranched polyglycerol, J. Am. Chem. Soc. 135 (2013) 8770–8773, https://doi.org/10.1021/ja400636d.

[23] P. Shi, N. Zhao, J. Lai, J. Coyne, E.R. Gaddes, Y. Wang, Polyvalent display of biomolecules on live cells, Angew. Chem. Int. Ed. 57 (2018) 6800–6804, https://doi.org/10.1002/anie.201712596.

[24] M.C. Arno, Engineering the mammalian cell surface with synthetic polymers: strategies and applications, Macromol. Rapid Commun. 41 (2020) 2000302, https://doi.org/10.1002/marc.202000302.

[25] S. Zhang, W. Li, J. Luan, A. Srivastava, V. Carnevale, M.L. Klein, J. Sun, D. Wang, S. P. Teora, S.J. Rijpkema, J.D. Meeldijk, D.A. Wilson, Adaptive insertion of a hydrophobic anchor into a poly(ethylene glycol) host for programmable surface functionalization, Nat. Chem. 15 (2023) 240–247, https://doi.org/10.1038/s41557-022-01090-0.

[26] J. Kim, J.M. An, Y. Jung, N.H. Kim, Y. Kim, D. Kim, Red-emitting SBBF (single-benzene-based fluorophore)-silica hybrid material: one-Pot synthesis, characterization, and biomedical applications, Nanomaterials 11 (2021) 2036, https://doi.org/10.3390/nano11082036.

[27] N. Tarannum, T.J. Hossain, F. Ali, T. Das, K. Dhar, I.H. Nafiz, Antioxidant, antimicrobial and emulsification properties of exopolysaccharides from lactic acid bacteria of bovine milk: insights from biochemical and genomic analysis, LWT 186 (2023) 115263, https://doi.org/10.1016/j.lwt.2023.115263.

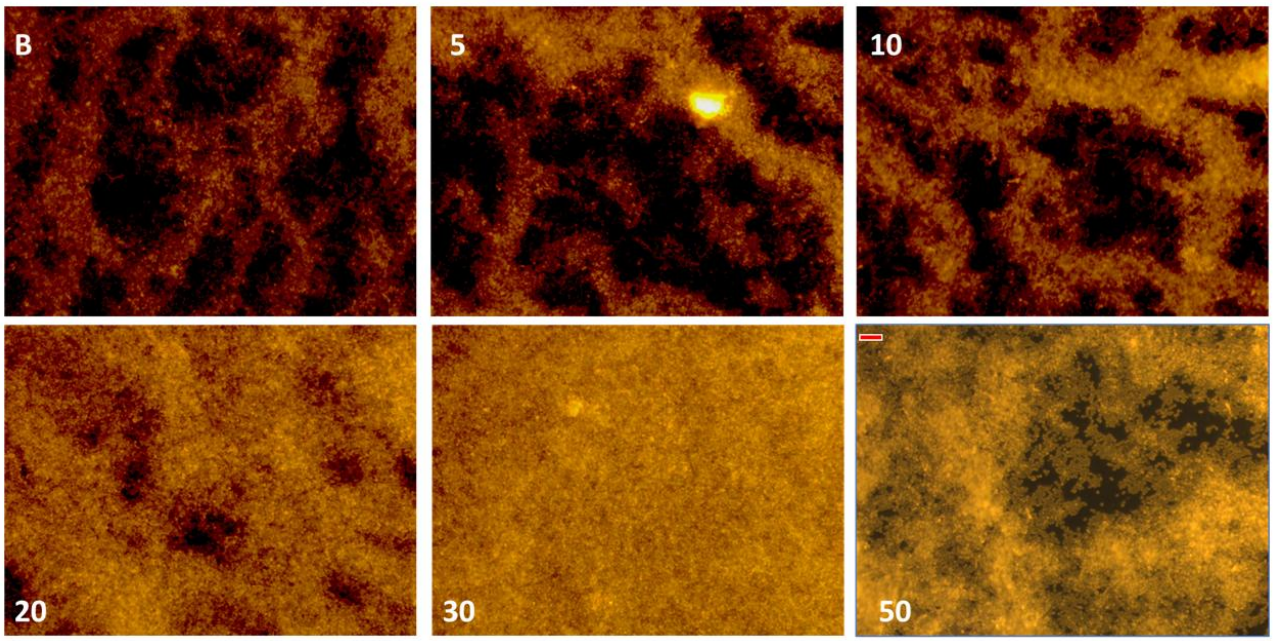
[28] H.A. Chung, K. Kato, C. Itoh, S. Ohhashi, T. Nagamune, Casual cell surface remodeling using biocompatible lipid-poly(ethylene glycol)(*n*): development of stealth cells and monitoring of cell membrane behavior in serum-supplemented conditions, J. Biomed. Mater. Res. 70A (2004) 179–185, https://doi.org/10.1002/jbm.a.20117.

[29] F. Frešer, G. Hostnik, J. Tošović, U. Bren, Dependence of the Fe(II)-Gallic acid coordination compound formation constant on the pH, Foods 10 (2021) 2689, https://doi.org/10.3390/foods10112689.

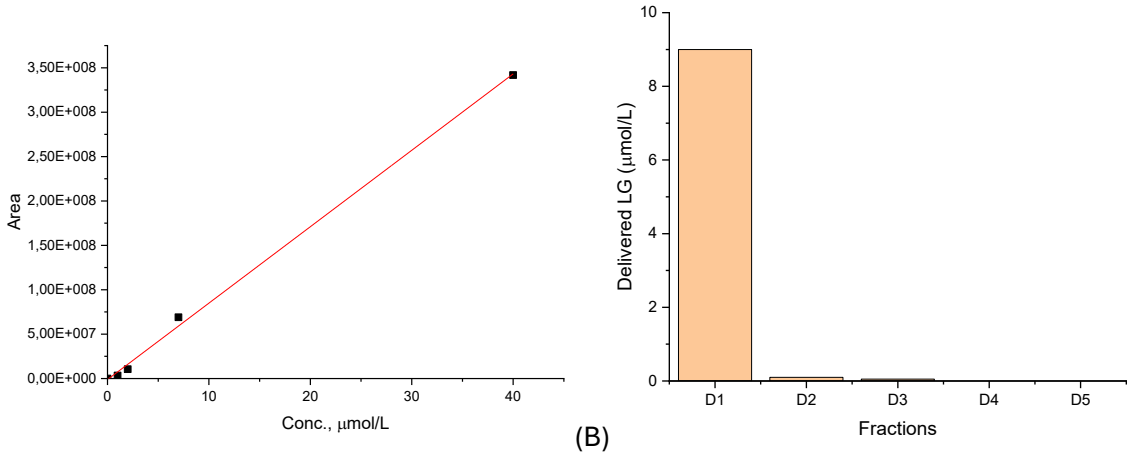
[30] R. Nishiyabu, Y. Kubo, T.D. James, J.S. Fossey, Boronic acid building blocks: tools for sensing and separation, Chem. Commun. 47 (2011) 1106, https://doi.org/10.1039/c0cc02920c.

[31] M.F. Fernandez, S. Boris, C. Barbes, Probiotic properties of human lactobacilli strains to be used in the gastrointestinal tract, J. Appl. Microbiol. 94 (2003) 449–455, https://doi.org/10.1046/j.1365-2672.2003.01850.x.
[32] V. D'Amico, I. Arduino, M. Vacca, R.M. Iacobazzi, D. Altamura, A. Lopalco, R. Rizzi, A. Cutrignelli, V. Laquintana, F. Massimo, M. De Angelis, N. Denora, A. A. Lopedota, Colonic budesonide delivery by multistimuli alginate/Eudragit® FS 30D/inulin-based microspheres as a paediatric formulation, Carbohydr. Polym. 302 (2023) 120422, https://doi.org/10.1016/j.carbpol.2022.120422.
[33] I. Kubo, N. Masuoka, P. Xiao, H. Haraguchi, Antioxidant activity of dodecyl Gallate, J. Agric. Food Chem. 50 (2002) 3533–3539, https://doi.org/10.1021/jf011250h.
[34] M. Donnaloia, F. De Mastro, C. Porfido, M.M. Giangregorio, R. Terzano, G. Brunetti, D. Vona, Chemically functionalized Eggs capsules of Sea Snail (ess) banded dye-murex for bioremediation applications, Environ. Chem. Ecotoxicol. 7 (2025) 644–654, https://doi.org/10.1016/j.enceco.2025.03.009.
[35] L. Savi, P. Leal, T. Vieira, R. Rosso, R. Nunes, R. Yunes, T. Creczynski-Pasa, C. Barardi, C. Simões, Evaluation of anti-herpetic and antioxidant activities, and cytotoxic and genotoxic effects of synthetic alkyl-esters of Gallic acid, Arzneimittelforschung 55 (2011) 66–75, https://doi.org/10.1055/s-0031-1296825.
[36] A. Sevanian, P. Hochstein, Mechanisms and consequences of lipid peroxidation in biological systems, Annu. Rev. Nutr. 5 (1985) 365–390.
[37] M. Jurak, R. Mroczka, R. Łopucki, Properties of artificial phospholipid membranes containing lauryl gallate or cholesterol, J. Membr. Biol. 251 (2018) 277–294, https://doi.org/10.1007/s00232-018-0025-z.
[38] EFSA Panel on Food additives and Nutrient Sources added to Food (ANS), Scientific Opinion on the re-evaluation of dodecyl gallate (E 312) as a food additive, in: EFS2 13, 2015, https://doi.org/10.2903/j.efsa.2015.4086.
[39] Scientific Opinion on the re-evaluation of octyl gallate (E 311) as a food additive, n. d. EFSA J.. doi:https://doi.org/10.2903/j.efsa.2015.4248.
[40] K. Yang, L. Zhang, P. Liao, Z. Xiao, F. Zhang, D. Sindaye, Z. Xin, C. Tan, J. Deng, Y. Yin, B. Deng, Impact of Gallic acid on gut health: focus on the gut microbiome, immune response, and mechanisms of action, Front. Immunol. 11 (2020) 580208, https://doi.org/10.3389/fimmu.2020.580208.
[41] B. Tian, P. Ye, X. Zhou, J. Hu, P. Wang, M. Cai, K. Yang, P. Sun, X. Zou, Gallic acid ameliorated chronic DSS-induced colitis through gut microbiota modulation, intestinal barrier improvement, and inflammation, Mol. Nutr. Food Res. 69 (2025) e70024, https://doi.org/10.1002/mnfr.70024.
[42] X. Wang, Q. Wang, Y. Hu, F. Yin, X. Liu, D. Zhou, Gastrointestinal digestion and microbial hydrolysis of alkyl gallates: potential sustained release of gallic acid, Foods 11 (2022) 3936, https://doi.org/10.3390/foods11233936.
[43] D. Zhan, Z. Bian, H. Li, R. Wang, G. Fang, Q. Yao, Z. Wu, Novel detection method for gallic acid: a water soluble boronic acid-based fluorescent sensor with double recognition sites, Bioorg. Med. Chem. Lett. 57 (2022) 128483, https://doi.org/10.1016/j.bmcl.2021.128483.
[44] F. Bayard, X. Chen, J.M. García-Arcos, A. Roux, N. Sakai, S. Matile, Hydrophobic interfacing of fluorescent membrane probes, ChemistryEurope 1 (2023) e202300041, https://doi.org/10.1002/ceur.202300041.
[45] I.Y. Tóth, M. Szekeres, R. Turcu, S. Sáringer, E. Illés, D. Nesztor, E. Tombácz, Mechanism of in situ surface polymerization of gallic acid in an environmental-inspired preparation of carboxylated core–shell magnetite nanoparticles, Langmuir 30 (2014) 15451–15461, https://doi.org/10.1021/la5038102.
[46] H. Luo, J. Xie, X. Su, P. Wang, H. Chen, X. Kuang, J. Liu, Tannic acid-based metal-phenolic networks as a versatile platform to mediate cell therapy, Sci. China-Mater. 67 (2024) 3833–3848, https://doi.org/10.1007/s40843-024-3139-3.
[47] J.H. Park, K. Kim, J. Lee, J.Y. Choi, D. Hong, S.H. Yang, F. Caruso, Y. Lee, I.S. Choi, A cytoprotective and degradable metal–polyphenol nanoshell for single-cell encapsulation, Angew. Chem. Int. Ed. 53 (2014) 12420–12425, https://doi.org/10.1002/anie.201405905.
[48] S.Y. Han, D.T. Nguyen, B.J. Kim, N. Kim, E.K. Kang, J.H. Park, I.S. Choi, Cytoprotection of probiotic lactobacillus acidophilus with artificial nanoshells of nature-derived eggshell membrane hydrolysates and coffee melanoidins in single-cell nanoencapsulation, Polymers 15 (2023) 1104, https://doi.org/10.3390/polym15051104.
[49] H. Lee, J. Park, S.Y. Han, S. Han, W. Youn, H. Choi, G. Yun, I.S. Choi, Ascorbic acid-mediated reductive disassembly of Fe^{3+} –tannic acid shells in degradable single-cell nanoencapsulation, Chem. Commun. 56 (2020) 13748–13751, https://doi.org/10.1039/D0CC05856D.
[50] Chamila P. Manankandayalage, Daniel K. Unruh, Clemens Krempner, Boronic, diboronic and boric acid esters of 1,8-naphthalenediol – synthesis, structure and formation of boronium salts, Dalton Trans. (2020) 4834–4842.
[51] D. Plamada, D.C. Vodnar, Polyphenols—gut microbiota interrelationship: a transition to a new generation of prebiotics, Nutrients 14 (2021) 137, https://doi.org/10.3390/nu14010137.
[52] R. Tabasco, F. Sánchez-Patán, M. Monagas, B. Bartolomé, M. Victoria Moreno-Arribas, C. Peláez, T. Requena, Effect of grape polyphenols on lactic acid bacteria and bifidobacteria growth: resistance and metabolism, Food Microbiol. 28 (2011) 1345–1352, https://doi.org/10.1016/j.fm.2011.06.005.
[53] J. Pan, G. Gong, Q. Wang, J. Shang, Y. He, C. Catania, D. Birnbaum, Y. Li, Z. Jia, Y. Zhang, N.S. Joshi, J. Guo, A single-cell nanocoating of probiotics for enhanced amelioration of antibiotic-associated diarrhea, Nat. Commun. 13 (2022) 2117, https://doi.org/10.1038/s41467-022-29672-z.
[54] R. Zhao, T. Yu, J. Li, R. Niu, D. Liu, W. Wang, Single-cell encapsulation systems for probiotic delivery: armor probiotics, Adv. Colloid Interf. Sci. 332 (2024) 103270, https://doi.org/10.1016/j.cis.2024.103270.
[55] X. Zhou, Q. Guo, M. Guo, B. Li, W. Peng, D. Wang, D. Ming, B. Zheng, Nanoarmour-shielded single-cell factory for bacteriotherapy of Parkinson's disease, J. Control. Release 338 (2021) 742–753, https://doi.org/10.1016/j.jconrel.2021.09.009.
[56] F. Centurion, S. Merhebi, M. Baharfar, R. Abbasi, C. Zhang, M. Mousavi, W. Xie, J. Yang, Z. Cao, F. Allioux, G.F.S. Harm, J. Biazik, K. Kalantar-Zadeh, Md.A. Rahim, Cell-mediated biointerfacial phenolic assembly for probiotic nano encapsulation, Adv. Funct. Mater. 32 (2022) 2200775, https://doi.org/10.1002/adfm.202200775.
[57] A. Xie, H. Ji, Z. Liu, Y. Wan, X. Zhang, H. Xiong, S.-P. Nie, H. Wan, Modified prebiotic-based "shield" armed probiotics with enhanced resistance of gastrointestinal stresses and prolonged intestinal retention for synergistic alleviation of colitis, ACS Nano 17 (2023) 14775–14791, https://doi.org/10.1021/acsnano.3c02914.
[58] L. Zhu, T. Yu, W. Wang, T. Xu, W. Geng, N. Li, X. Zan, Responsively degradable nanoarmor-assisted super resistance and stable colonization of probiotics for enhanced inflammation-targeted delivery, Adv. Mater. 36 (2024) 2308728, https://doi.org/10.1002/adma.202308728.
[59] M. De Angelis, S. Siragusa, M. Vacca, R. Di Cagno, F. Cristofori, M. Schwarm, S. Pelzer, M. Flügel, B. Speckmann, R. Francavilla, M. Gobbetti, Selection of gut-resistant bacteria and construction of microbial consortia for improving gluten digestion under simulated gastrointestinal conditions, Nutrients 13 (2021) 992, https://doi.org/10.3390/nu13030992.
[60] K. Papadimitriou, Á. Alegría, P.A. Bron, M. De Angelis, M. Gobbetti, M. Kleerebezem, J.A. Lemos, D.M. Linares, P. Ross, C. Stanton, F. Turroni, D. Van Sinderen, P. Varmanen, M. Ventura, M. Zúñiga, E. Tsakalidou, J. Kok, Stress physiology of lactic acid bacteria, Microbiol. Mol. Biol. Rev. 80 (2016) 837–890, https://doi.org/10.1128/MMBR.00076-15.
[61] M. Vacca, G. Celano, N. Serale, G. Costantino, F.M. Calabrese, M. Calasso, M. De Angelis, Dynamic microbial and metabolic changes during Apulian Caciocavallo cheesemaking and ripening produced according to a standardized protocol, J. Dairy Sci. 107 (2024) 6541–6557, https://doi.org/10.3168/jds.2023-24049.
[62] M. Alves Gragnani Vido, I. Dutra Alvim, G. Vinderola, M. Isabel Berto, P. Blumer Zacarchenco Rodrigues De Sá, C. Mauricio Barreto Pinilla, A. Torres Silva E Alves, Microencapsulation of Limosilactobacillus reuteri (DSM 23878) for application in infant formula: heat resistance and bacterial viability during long-time storage, Food Res. Int. 173 (2023) 113378, https://doi.org/10.1016/j.foodres.2023.113378.
[63] B. Liu, J. Hu, H. Yao, L. Zhang, H. Liu, Improved viability of probiotics encapsulated by layer-by-layer assembly using zein nanoparticles and pectin, Food Hydrocoll. 143 (2023) 108899, https://doi.org/10.1016/j.foodhyd.2023.108899.
[64] S. Ge, J. Han, Q. Sun, Q. Zhou, Z. Ye, P. Li, Q. Gu, Research progress on improving the freeze-drying resistance of probiotics: a review, Trends Food Sci. Technol. 147 (2024) 104425, https://doi.org/10.1016/j.tifs.2024.104425.
[65] H.W. Tang, S. Abbasiliasi, P. Murugan, Y.J. Tam, H.S. Ng, J.S. Tan, Influence of freeze-drying and spray-drying preservation methods on survivability rate of different types of protectants encapsulated *Lactobacillus acidophilus* FTDC 3081, Biosci. Biotechnol. Biochem. 84 (2020) 1913–1920, https://doi.org/10.1080/09168451.2020.1770572.
[66] N.E. Buitimea-Cantúa, J.A. Gutiérrez-Uribe, S.O. Serna-Saldívar, Phenolic–protein interactions: effects on food properties and health benefits, J. Med. Food 21 (2018) 188–198, https://doi.org/10.1089/jmf.2017.0057.
[67] F. Shahidi, K.D. Athiyappan, Polyphenol-polysaccharide interactions: molecular mechanisms and potential applications in food systems – a comprehensive review, Food Prod. Process. Nutr. 7 (2025) 42, https://doi.org/10.1186/s43014-025-00322-3.
[68] E. Nemli, G. Ozkan, B. Gultekin Subasi, H. Cavdar, J.M. Lorenzo, C. Zhao, E. Capanoglu, Interactions between proteins and phenolics: effects of food processing on the content and digestibility of phenolic compounds, J. Sci. Food Agric. 104 (2024) 2535–2550, https://doi.org/10.1002/jsfa.13275.
[69] T. Zhang, C. Wang, T. Du, H. Sun, Y. Han, S. Shi, J. Wang, W. Zhang, Polydopamine-mediated biointerfacial nanozyme as probiotic protective coating for IBD therapy, Int. J. Biol. Macromol. 308 (2025) 142699, https://doi.org/10.1016/j.ijbiomac.2025.142699.
[70] Q. Song, H. Zhao, C. Zheng, K. Wang, H. Gao, Q. Feng, H. Zhang, Z. Zhang, Y. Zhang, L. Wang, A bioinspired versatile spore coat nanomaterial for oral probiotics delivery, Adv. Funct. Mater. 31 (2021) 2104994, https://doi.org/10.1002/adfm.202104994.

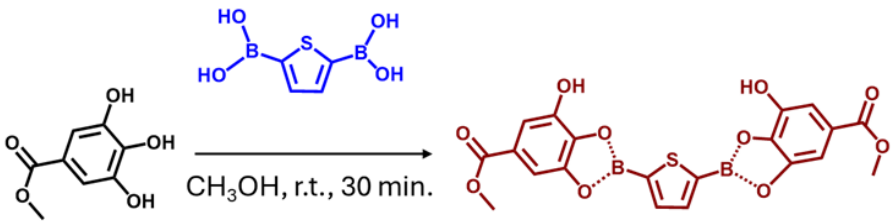
Supplementary material

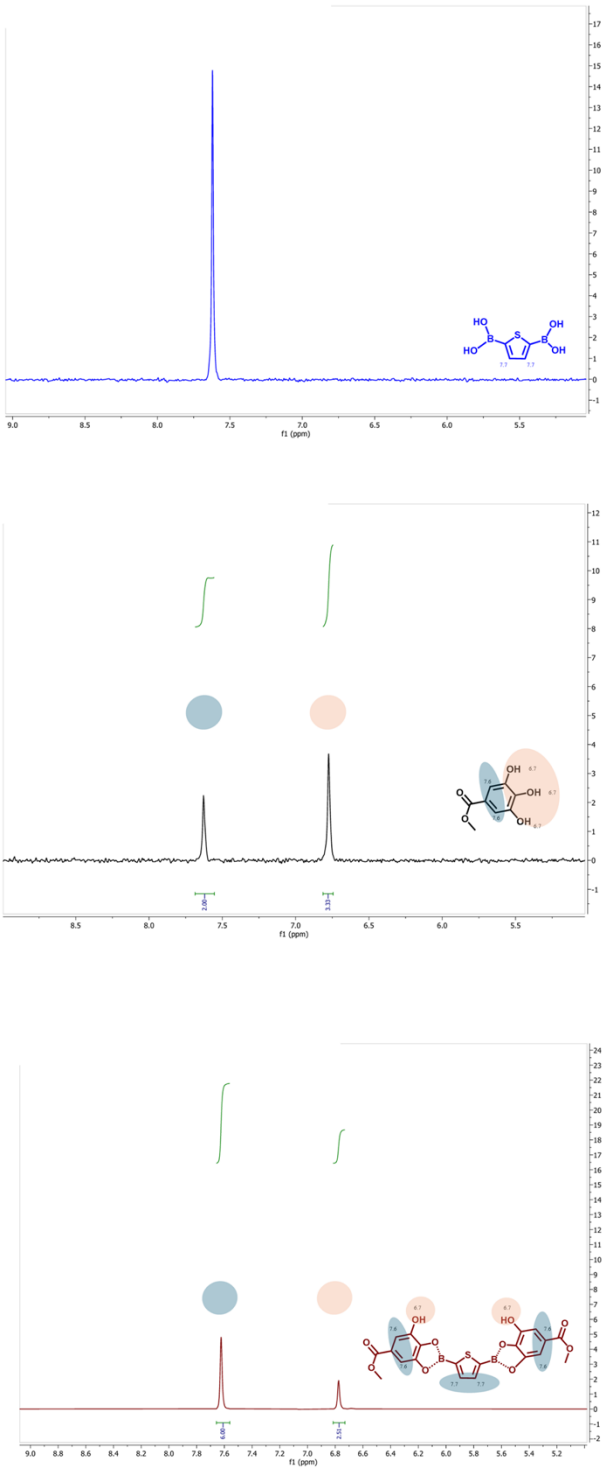


Supp. Figure S1| Visualization under fluorescence bidimensional microscopy of bare bacteria and hydrophobically LG-inserted bacteria (5, 10, 20, 30, 50 µM) after incubation with f boronic sensor molecule (scale bar: 50 µm).



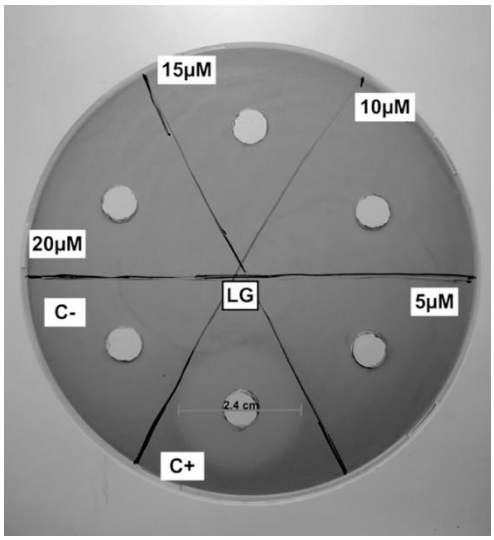
Supp. Figure S2| (a) Calibration curve for LG in the range of 0-40 µmol/L; (b) histograms reporting outputs in delivered LG for D1-D5 fractions (1, 2, 4, 8, 12 hours, respectively).



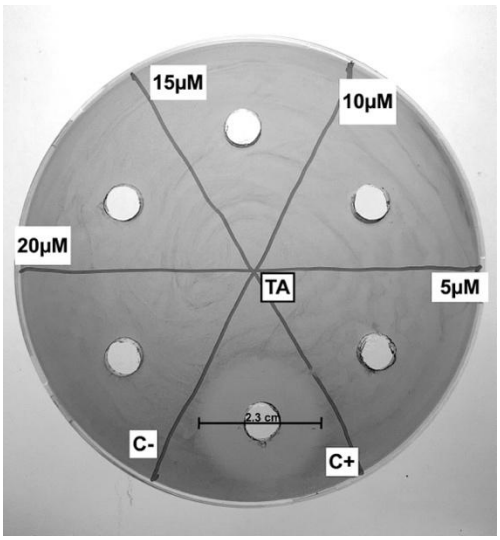


Supp. Figure S3| In batch solution reaction of esterification between bis-boronic tiophene moiety and gallic acid methyl ester. Single ^{1}H-NMR have been reported here.

a)



b)



Supp. Figure S4| Evaluation of the antimicrobial effect, by diffusion assay on agar plates, of (a) the lauryl gallate (LG) monomer and (b) the tannin-like acid (TA) polymer used at different concentrations (5–20µM). C+ and C- represent the positive (chloramphenicol) and negative (water) control, respectively.